OPEN

see commentary on page 234

Adventitial transduction of lentivirus-shRNA-VEGF-A in arteriovenous fistula reduces venous stenosis formation

Binxia Yang[1,5], Rajiv Janardhanan[1,5], Pawan Vohra[1], Eddie L. Greene[2], Santanu Bhattacharya[1], Sarah Withers[1], Bhaskar Roy[1], Evelyn C. Nieves Torres[1], Jaywant Mandrekar[3], Edward B. Leof[4], Debabrata Mukhopadhyay[4] and Sanjay Misra[1,4]

[1]*Vascular and Interventional Radiology Translational Laboratory, Department of Radiology, Mayo Clinic, Rochester, Minnesota, USA;* [2]*Division of Nephrology and Hypertension, Mayo Clinic, Rochester, Minnesota, USA;* [3]*Department of Biostatistics, Mayo Clinic, Rochester, Minnesota, USA and* [4]*Department of Biochemistry and Molecular Biology, Mayo Clinic, Rochester, Minnesota, USA*

Venous neointimal hyperplasia (VNH) causes hemodialysis vascular access failure. Here we tested whether VNH formation occurs in part due to local vessel hypoxia caused by surgical trauma to the vasa vasorum of the outflow vein at the time of arteriovenous fistula placement. Selective targeting of the adventitia of the outflow vein at the time of fistula creation was performed using a lentivirus-delivered small-hairpin RNA that inhibits VEGF-A expression. This resulted in significant increase in mean lumen vessel area, decreased media/adventitia area, and decreased constrictive remodeling with a significant increase in apoptosis (increase in caspase 3 activity and TUNEL staining) accompanied with decreased cellular proliferation and hypoxia-inducible factor-1α at the outflow vein. There was significant decrease in cells staining positive for α-smooth muscle actin (a myofibroblast marker) and VEGFR-1 expression with a decrease in MMP-2 and MMP-9. These results were confirmed in animals that were treated with humanized monoclonal antibody to VEGF-A with similar results. Since hypoxia can cause fibroblast to differentiate into myofibroblasts, we silenced VEGF-A gene expression in fibroblasts and subjected them to hypoxia. This decreased myofibroblast production, cellular proliferation, cell invasion, MMP-2 activity, and increased caspase 3. Thus, VEGF-A reduction at the time of arteriovenous fistula placement results in increased positive vascular remodeling.

Kidney International (2014) **85,** 289–306; doi:10.1038/ki.2013.290; published online 7 August 2013

KEYWORDS: diabetes; vascular access; VEGF

Correspondence: *Sanjay Misra, Department of Radiology, Mayo Clinic, 200 First Street SW, Rochester, Minnesota, 55905, USA.*
E-mail: misra.sanjay@mayo.edu

[5]These authors contributed equally to this work.

Received 19 November 2012; revised 2 June 2013; accepted 20 June 2013; published online 7 August 2013

More than 400,000 patients have end-stage renal disease and require chronic hemodialysis in the United States.[1] Vascular access through an arteriovenous fistula (AVF) is required for the optimal hemodialysis and clearance of uremic toxins. AVF failure occurs frequently because of venous stenosis formation, and the patency of AVFs at 1 year is estimated to be only 62%.[2] Over a billion dollars are spent annually to maintain the function of hemodialysis AVFs and grafts.[1] Angioplasty is the current treatment for treating venous stenosis formation, and noninvasive treatments that could reduce AVF stenosis would be advantageous to end-stage renal disease patients.

Venous neointimal hyperplasia (VNH) causes venous stenosis formation to occur in AVFs.[3] When specimens removed from patients with failed AVFs are examined using histologic techniques, changes in angiogenesis are observed within the neointima and adventitia of the vessel. This is often accompanied with increased proliferation of cells that are α-smooth muscle actin (α-SMA) positive located within the neointima.[4–6] There are emerging experimental data demonstrating that adventitial and medial cells, which are hypothesized to be fibroblasts, will convert to myofibroblasts (α-SMA-positive cells) and thus contribute to the formation of VNH.[7–10] *In vitro* studies indicate that hypoxia causes increased differentiation of fibroblasts to myofibroblasts, whereas increased expression of hypoxia-inducible factor-1α (HIF-1α) has been observed *in vivo* in both animal models of hemodialysis AVF and graft failure, as well as in specimens removed from patients with hemodialysis AVF or graft failure.[7,11–14] One plausible explanation for these observations is that the vasa vasorum supplying the vessel wall becomes disrupted after the surgical placement of the AVF. Taken collectively, these observations suggest that hypoxia-driven angiogenic stimuli enhance matrix deposition while facilitating the conversion of adventitial fibroblasts to myofibroblasts.[4] Therefore, a therapy aimed at reducing hypoxia-driven VNH would be useful in reducing stenosis in AVFs. An ideal therapy to reduce venous stenosis formation would be one that can be delivered selectively to the

adventitia of the vessel wall where it might target the resident fibroblasts. This directed approach to therapy might have several advantages over systemically delivered therapies because of higher local concentrations of the drug owing to direct delivery and reduced clearance by other organs, lower systemic side effects, and a reduced chance for nontarget delivery to other vessels or organs.

Vascular endothelial growth factor-A (*VEGF-A*) is one of the most potent angiogenic factors, and its action is mediated through its two receptors: *VEGFR-1* (fms-related tyrosine kinase-1 (Flt-1)) and *VEGFR-2* (fetal liver kinase-2 (Flk-2)). *VEGF-A* is important in vascular remodeling and it has been shown to be involved in the pathogenesis of arterial stenosis, vein bypass grafts, and VNH associated with hemodialysis vascular access.[6,15–22] Previous work from our and other laboratories has demonstrated that there is increased expression of *VEGF-A*, *VEGFR-1*, and *VEGFR-2* at the site of venous stenosis in murine and porcine models of hemodialysis AVF and graft failure. Recent work from our laboratory has shown that simvastatin treatment before the placement of AVF reduces VNH formation in a murine model of chronic kidney disease with AVF by decreasing VEGF-A and matrix metalloproteinase (*MMP-9*).[10] This study did not determine the mechanism by which *VEGF-A* has a role in VNH formation, as simvastatin has been implicated in reducing many different cytokines.[13,14,23]

Experiments outlined in this study were performed in a murine model of chronic kidney disease with AVF to test the hypothesis that reduction of *VEGF-A* gene expression by adventitial delivery to the outflow vein of the AVF at the time of placement would lead to a reduction in several important downstream matrix regulating genes such as *MMP-2* and *MMP-9*, and thereby reduces VNH and abnormal vascular remodeling. Gene expression for *VEGF-A* was reduced by adventitial delivery of a small hairpin RNA (shRNA) that inhibits *VEGF-A* expression. Gene, protein expression, and histomorphometric analyses were performed at the outflow vein after administration of anti-*VEGF-A* RNA therapy. We determined whether Avastin, a humanized monoclonal antibody to *VEGF-A* (Bevacizumab, Genentech, San Francisco, CA), would decrease VNH formation. Finally, we investigated whether *VEGF-A* expression induced by hypoxia resulted in myofibroblast formation by silencing *VEGF-A* gene expression in fibroblasts and subjecting them to hypoxia for different time periods, and subsequently determined the rates of protein expression, cell proliferation, and migration.

RESULTS

Surgical outcomes

A total of 204 male C57BL/6 mice weighing 25–30 g underwent right nephrectomy and left upper pole occlusion surgery, as described previously.[10] One mouse was used to perform micro-computed tomography analysis to evaluate the vasa vasorum.

In all, 7 mice died after nephrectomy, 4 after AVF fistula placement, and 16 had significant arterial thickening and inflammation such that a new AV fistula could not be placed. A total of 140 mice underwent placement of an AVF to connect the right carotid artery to the ipsilateral jugular vein.[10] Next, either 1×10^6 particle-forming units (PFU) of lentivirus (LV)-shRNA-*VEGF-A* (LV, $n=72$) or scrambled-shRNA-*VEGF-A* (control (C), $n=68$) were injected into the adventitia of the outflow vein where the stenosis forms in this model.[23,24] Animals were killed for gene expression, protein, or histologic analyses at days 3, 7 14, 21, and 28 after AVF placement. At the time of killing, the fistula was evaluated for patency. The fistula was considered to be patent if, when the outflow vein was compressed, it became dilated under visual inspection. A separate group of 36 animals underwent treatment with Avastin (5 mg/kg) or immunoglobulin G (IgG) isotype–matched antibody in equal volume of phosphate-buffered saline (PBS) administered intraperitoneally every other day, which was started 1 week before fistula placement and continued up to the time of killing. Animals were killed on day 7 for gene expression of *VEGF-A* and on days 14 and 28 after AVF placement for histomorphometric analysis.

Figure 1 | Vascular endothelial growth factor-A (*VEGF-A*) expression is reduced in lentivirus (LV)–small hairpin RNA (shRNA)-*VEGF-A*-transduced and Avastin-treated vessels with decreased CD31 staining. (**a**, first to third columns) *In situ* hybridization of mRNA for *VEGF-A* in the LV-transduced vessels when compared with scrambled-shRNA-*VEGF-A* (control (C)) vessels, with arrows on cells positive for *VEGF-A* mRNA expression (brown). By day 3 (D3), there was a reduction of mRNA for *VEGF-A* being localized to the media and adventitia and by day 7 (D7), it was localized to the media and intima. In contrast, the vessels transduced with C shRNA showed increased mRNA expression of *VEGF-A* in the adventitia and media by day 3, and in the media and intima by day 7. (**b**) Pooled data for the *in situ* transcript levels of *VEGF-A* in the outflow vein of the LV-transduced vessels that was significantly reduced when compared with C vessels at day 7 ($P<0.0001$). (**c**) Upper panel shows the representative real-time PCR (RT-PCR) blots of the *VEGF-A* with *18S* gene for loading with pooled data from the mean gene expression of *VEGF-A* using RT-PCR analysis. This demonstrates that there is significant reduction in the mean *VEGF-A* expression in the LV-transduced vessels when compared with C vessels at day 7 ($P<0.0001$). (**d**) Representative sections from *VEGF-A* staining at the venous stenosis of the LV and C-transduced vessels or Avastin-treated or immunoglobulin G (IgG) controls at days 14 and 28. At day 14, there is a significant reduction in the mean *VEGF-A* staining in the LV-transduced vessels and Avastin-treated vessels when compared with controls ($P<0.0001$). (**e**) Representative sections from CD31 staining at the venous stenosis of the LV and C-transduced vessels or Avastin-treated vessels or IgG controls at days 14 and 28. Cells staining brown are positive for CD-31. All are original magnification ×40. Bar = 200 μm. *Indicates the lumen. Qualitatively, in the C tissue, when compared with the LV-transduced vessels, there is increased CD31 staining localized to the neointima/media junction by days 14 to 28 in the control tissue. Similar results in the IgG control tissues when compared with Avastin-treated vessels. (**b**–**d**) Each bar shows mean ± s.e.m. of 4–6 animals per group. Two-way analysis of variance (ANOVA) followed by Student's *t*-test with *post hoc* Bonferroni's correction was performed. Significant difference from control value is indicated by $^{\#}P<0.0001$.

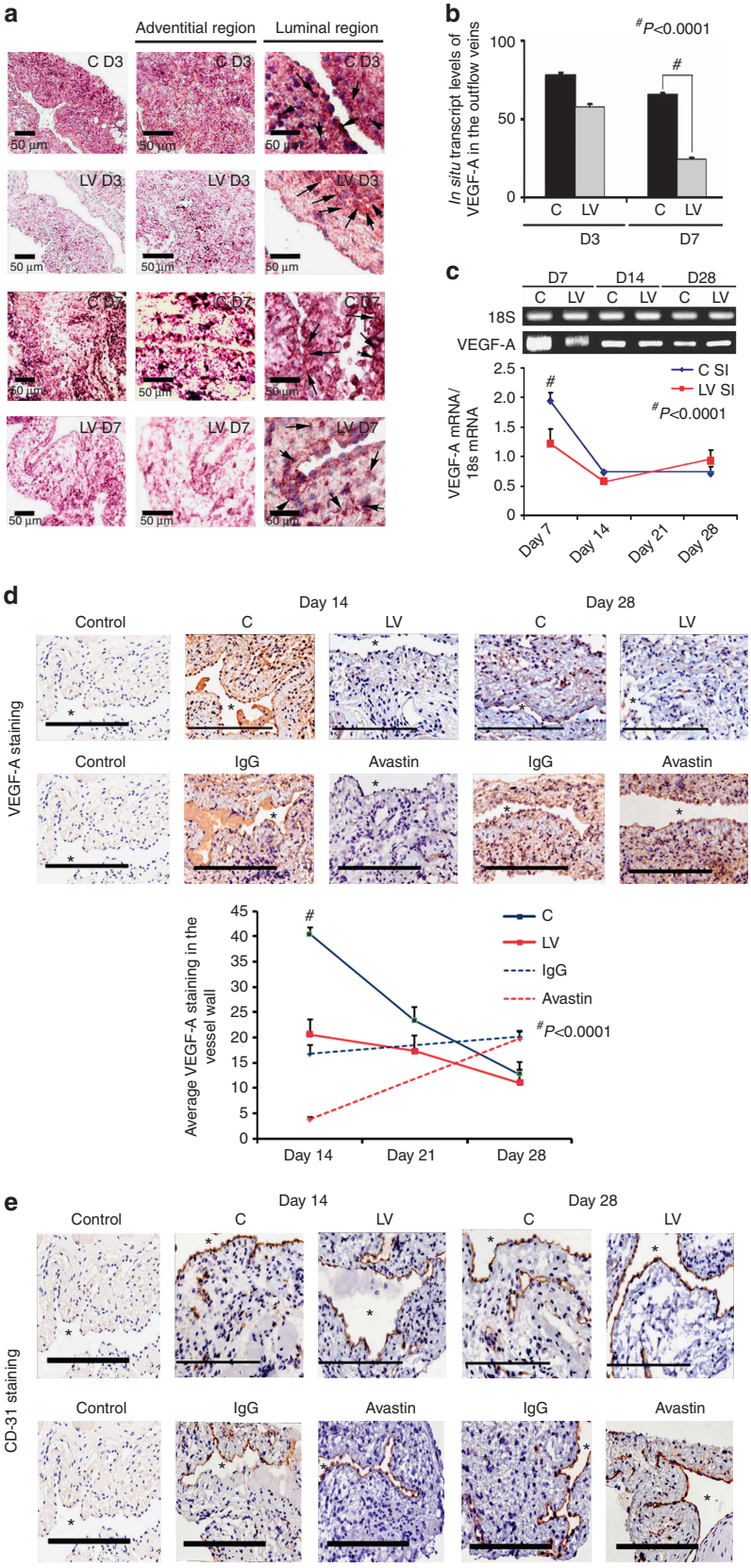
a
Adventitial region
Luminal region
C D3
LV D3
C D7
LV D7
50 μm
b
In situ transcript levels of VEGF-A in the outflow veins
#P<0.0001
C
LV
D3
D7
c
D7
D14
D28
18S
VEGF-A
VEGF-A mRNA/ 18s mRNA
C SI
LV SI
#P<0.0001
Day 7
Day 14
Day 21
Day 28
d
Day 14
Day 28
Control
IgG
Avastin
VEGF-A staining
Average VEGF-A staining in the vessel wall
#P<0.0001
e
CD-31 staining

Serum blood urea nitrogen (BUN) and creatinine after nephrectomy

In this model, we observed elevated creatinine and BUN levels similar to what is observed in the typical clinical scenario. The mean BUN and creatinine at baseline was 28 ± 5 and 0.26 ± 0.1 mg/dl, respectively. The mean BUN increased significantly at 5, 6, and 8 weeks after nephrectomy when compared with baseline ($P < 0.05$). In addition, there was no difference in the mean BUN and creatinine between the Avastin-treated or control animals.

Adventitial transduction of LV-shRNA-*VEGF-A* to the outflow vein reduces gene expression of *VEGF-A* at days 3 and 7 and *VEGF-A* staining until day 14

The efficacy of reducing *VEGF-A* gene expression *in vitro* was first determined in AKR-2B (murine fibroblast cell line) cells, which were transduced with either LV-shRNA-*VEGF-A* (LV) or scrambled shRNA-*VEGF-A* (C, control). Real-time PCR (RT-PCR) (Supplementary Figure S1A online) and western blot analyses (Supplementary Figure S1B online) demonstrated a greater than twofold decrease in *VEGF-A* expression in the LV-shRNA-*VEGF-A*-transduced cells when compared with controls. To ascertain whether similar findings are present *in vivo*, experiments were designed and performed to determine the distribution of the LV in the vasculature after delivery to the vessel wall.

The amount of reduction and localization of *VEGF-A* gene expression was determined *in vivo* using *in situ* hybridization for *VEGF-A*. By day 3, there was a reduction of mRNA for *VEGF-A* (brown staining in cells) being localized to the media and adventitia and, by day 7, it was localized to the media and intima (Figure 1a, first to third columns). In contrast, the vessels transduced with control shRNA showed increased mRNA expression of *VEGF-A* in the adventitia and media by day 3, and in the media and intima by day 7. Semiquantitative analysis of the *in situ* hybridization was performed, and it confirmed a significant reduction in the mRNA levels in the LV-shRNA-*VEGF-A*-transduced vessels when compared with control vessels by day 7 (24.5 ± 3.3 vs. 65.3 ± 6, respectively, $P < 0.0001$, average reduction: 62%, Figure 1b). Our next set of studies used RT-PCR analysis for *VEGF-A* on sections removed from the outflow vein at days 7, 14, and 28 after lentiviral transduction. By day 7, the mean gene expression of *VEGF-A* at the LV-shRNA-*VEGF-A*-transduced vessels was significantly lower than the control vessels (1.31 ± 0.17 vs. 1.96 ± 0.15, respectively, $P < 0.0001$, average reduction: 44%, Figure 1c), and by days 14 and 28 there was no difference in expression between the two groups ($P =$ not significant (NS)). Next, we determined the gene expression of *VEGF-A* in the Avastin-treated vessels when compared with controls at day 7. By day 7, we observed a significant reduction in *VEGF-A* expression in the Avastin-treated vessels when compared with controls (0.34 ± 0.05 vs. 0.67 ± 0.12, respectively; $P < 0.05$, average reduction: 49%).

The decrease in expression of the protein lags behind the decrease in gene expression. We determined the expression of *VEGF-A* after silencing using immunohistochemistry at days 14, 21, and 28 after LV silencing of *VEGF-A*. We observed a significant reduction in the average *VEGF-A* staining at day 14 in the LV-*VEGF-A*-transduced vessels when compared with controls (22.5 ± 2.7 vs. 40.4 ± 1.4, respectively, $P < 0.0001$, average reduction: 44%, Figure 1d). There was no difference at days 21 and 28 between the two groups. Finally, we determined the *VEGF-A* expression in the Avastin-treated vessels when compared with controls and observed similar findings. By day 14, there was a significant reduction in the average *VEGF-A* staining in the Avastin-treated vessels when compared with controls (3.8 ± 0.5 vs. 16.8 ± 1.8, respectively, $P < 0.0001$, average reduction: 77%, Figure 1d).

VEGF-A is responsible for angiogenesis, and it was assessed using CD31 staining. We observed qualitatively in the control vessels that, when compared with the LV-shRNA-*VEGF-A*-transduced vessels, there is increased CD31 staining with microvessel formation localized to the adventitia/media junction by days 14 to 28, which was associated with a reduced luminal vessel area (Figure 1e). Similar findings were observed in the Avastin-treated vessels when compared with controls.

Collectively, these results indicate that the reduction in mRNA was reduced in adventitia and media at day 3, and by day 7 it was in the media and intima following a 'top-down effect.' Taken collectively, these results indicate that mRNA levels of *VEGF-A* can be reduced at the outflow vein using adventitial delivery of LV-shRNA-*VEGF-A*, and the reduction in *VEGF-A* mRNA signal lasts for 1 week after delivery (Table 1). Moreover, *VEGF-A* staining shows a reduction in the VEGF-A protein expression until 2 weeks after both lentiviral delivery and Avastin treatment. There was a decrease in the CD31 staining in both the LV-shRNA-*VEGF-A*-transduced and Avastin-treated vessels when compared with controls.

Adventitial transduction of LV-shRNA-*VEGF-A* to the outflow vein promotes positive vascular remodeling with a decrease in constrictive remodeling

We hypothesized that reducing mRNA levels of *VEGF-A* by adventitial transduction of LV-shRNA-*VEGF-A* to the outflow vein or systemic delivery of Avastin would result in positive vascular remodeling at the outflow vein (Figure 2). We used hematoxylin and eosin staining (Figure 2a, first column) and picrosirius red staining (Figure 2a, second column) to assess the histomorphometric remodeling. A representative hematoxylin and eosin stain is shown from day 14. At days 14–28, there was a significant increase in the average lumen area of the outflow vein of the LV-shRNA-*VEGF-A*-transduced vessels when compared with the control vessels ($P < 0.001$ for days 14, 21, and 28, average increase: 175–290%, Figure 2b). In the Avastin-treated vessels, we observed a significant increase in the average lumen vessel area when compared with controls ($P < 0.01$ for day 14, average increase: 227%), with no difference by day 28.

Adventitial remodeling has been seen in experimental models of venous neointimal hyperplasia associated with

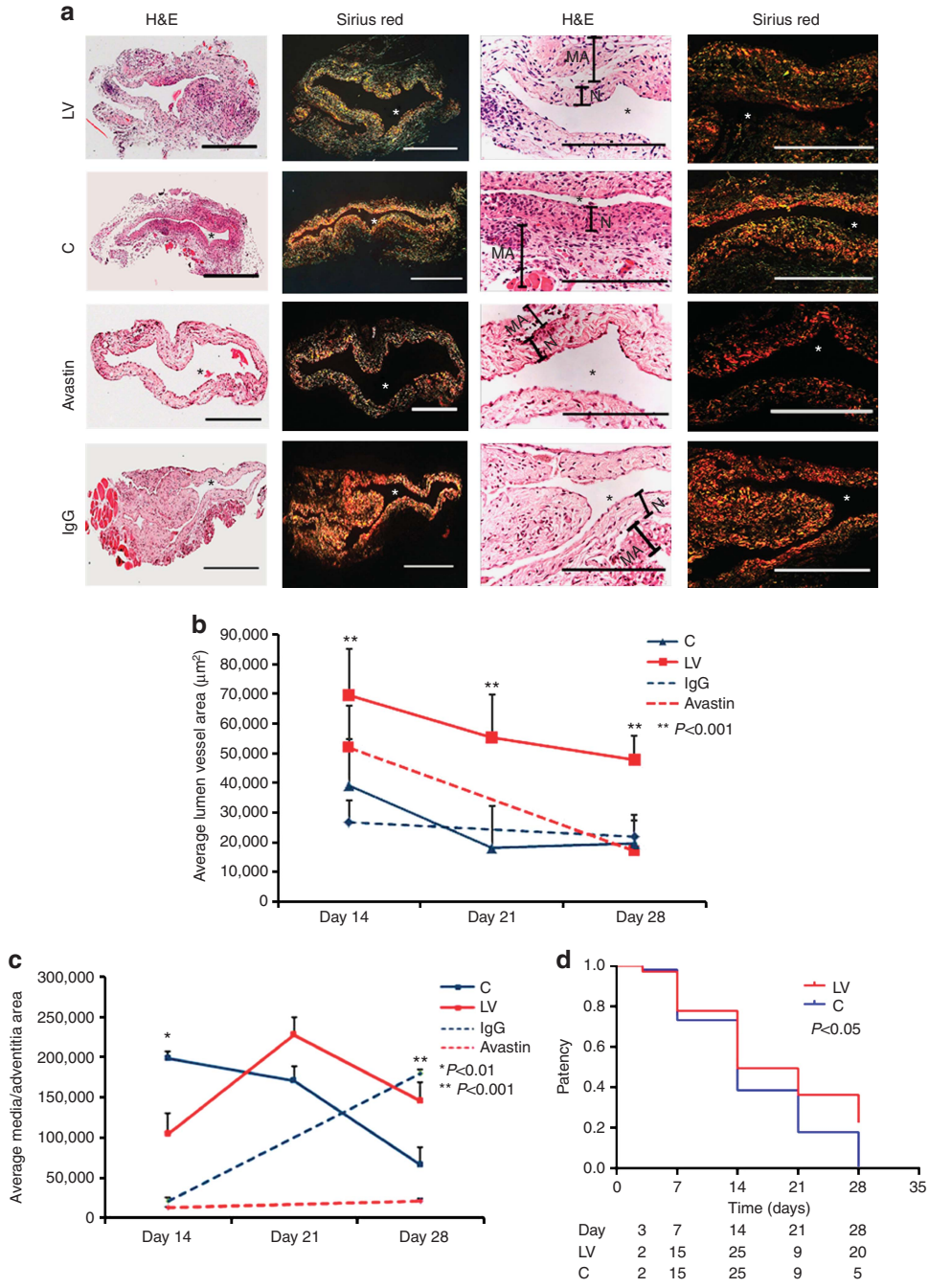

Figure 2 | Hematoxylin and eosin (H&E) and picrosirius red staining of the lentivirus (LV)–small hairpin RNA (shRNA)–vascular endothelial growth factor-A (*VEGF-A*)–transduced and Avastin-treated vessels have increased lumen vessel area with decreased media and adventitia area and collagen expression. (**a**, first column) Representative sections after H&E at the venous stenosis of the LV-shRNA-*VEGF-A* (LV) and scrambled-*VEGF-A* (control (C))–transduced vessels or Avastin-treated vessels or immunoglobulin G (IgG) controls at day 14 showing increase in lumen vessel area. (**a**, second column) Representative polarized light microscopy of picrosirius red–stained venous stenosis showing decreased fibrosis (collagen fibers are bright yellow) of the LV and C-transduced vessels and Avastin-treated vessels and controls. Qualitatively, there is a reduction in collagen staining by Sirius red by days 3–21. *Indicates the lumen. Bar = 200 μm. Pooled data for mean lumen vessel area LV and C groups and Avastin-treated and control vessels are shown in **b**. There is a significant increase in the mean lumen vessel area in the LV-transduced vessels when compared with C vessels for days 14–28 ($P<0.001$ for all). By day 14, there was a significant increase in the mean lumen vessel area in the Avastin-treated vessels when compared with IgG controls ($P<0.001$). Pooled data for mean media and adventitia area in LV and C groups and Avastin and control groups are shown in **c**. There is a significant decrease in the mean media and adventitia area in the LV-transduced vessels when compared with C vessels for day 14 ($P<0.01$). By day 28, there is a significant reduction in the mean media and adventitia area in the Avastin-treated vessels when compared with controls ($P<0.001$). (**d**) Kaplan–Meier estimates for LV-transduced vessels (red) when compared with C vessels (blue). There is improved patency in the LV-transduced vessels (red) when compared with C vessels (Log-rank test: $P<0.05$). (**b**, **c**) Each bar shows mean ± s.e.m. of 4–6 animals per group. Two-way analysis of variance (ANOVA) followed by Student's *t*-test with *post hoc* Bonferroni's correction was performed. Significant difference from control value is indicated by $^{**}P<0.001$.

hemodialysis vascular access.[7–9] We determined the area of the media and adventitia. By day 14, we observed a significant reduction in the average area of the media and adventitia of the LV-transduced vessels when compared with controls ($P<0.01$ for day 14, average decrease: 47%, Figure 2c), with gradual increase by days 21 and 28. In the

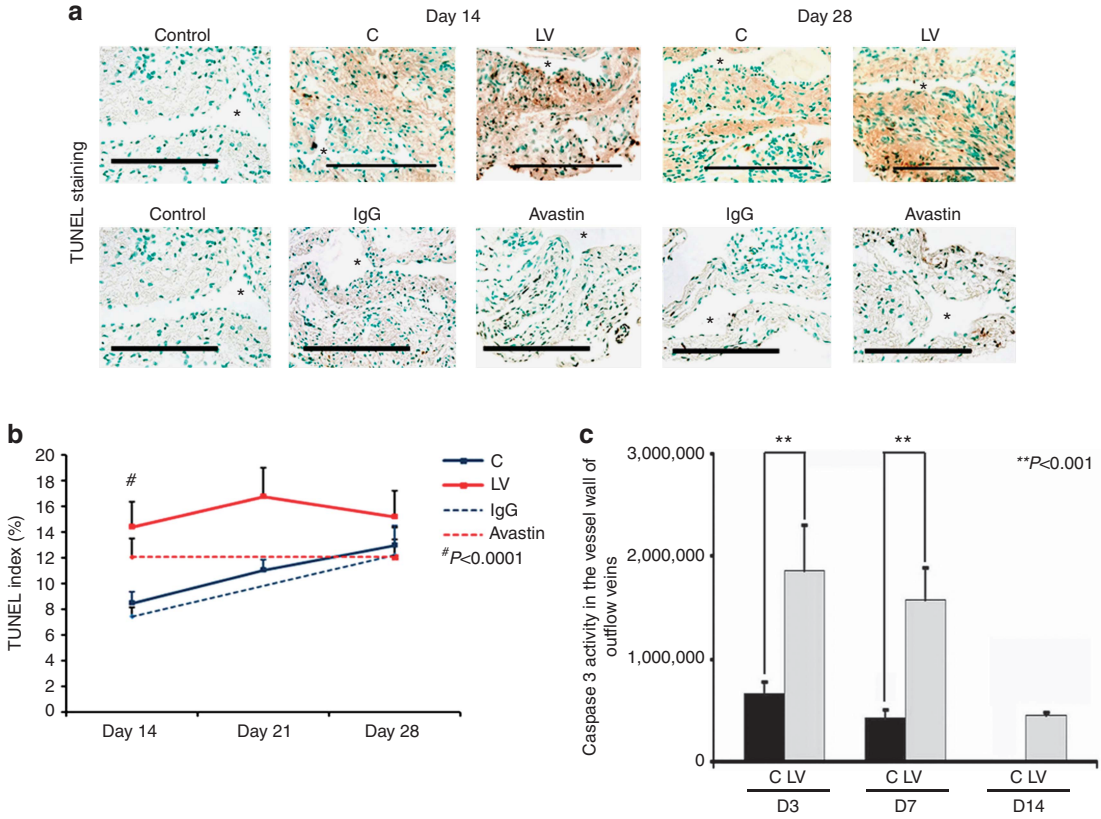

Figure 3 | (**a**) Representative sections from TdT-mediated dNTP nick end labeling (TUNEL) staining at the venous stenosis of the LV-shRNA-*VEGF-A* (LV) with scrambled-*VEGF-A* (control (C))–transduced control vessels or Avastin-treated with immunoglobulin G (IgG) controls at days 14 and 28. Nuclei staining brown are positive for TUNEL. Negative control is shown where the recombinant terminal deoxynucleotidyl transferase enzyme was omitted. All are original magnification ×40. Bar = 200 μm. *Indicates the lumen. Pooled data for LV- and C-transduced vessels or Avastin-treated or IgG controls are shown in **b**. This demonstrates a significant increase in the mean TUNEL index at day 14 ($P<0.0001$) in the LV group when compared with C group. Similar results are seen in Avastin-treated vessels when compared with IgG controls at day 14 ($P<0.0001$). Pooled data for the LV- and C-transduced vessels for caspase 3 activity at days 3 (D3), 7 (D7), and 14 (D14) is shown in **c**. This demonstrates a significant increase in the mean caspase 3 activities at days 3 to 14 (all $P<0.001$). Each bar shows mean ± s.e.m. of 3–6 animals per group (**b**, **c**). Two-way analysis of variance (ANOVA) followed by Student's *t*-test with *post hoc* Bonferroni's correction was performed. Significant difference from control value is indicated by $^{**}P<0.001$ and $^{\#}P<0.0001$.

Figure 4 | Cellular proliferation, matrix metalloproteinase 2 (*MMP-2*), and matrix metalloproteinase 9 (*MMP-9*) are decreased in lentivirus (LV)–small hairpin RNA (shRNA)–vascular endothelial growth factor-A (*VEGF-A*)–transduced vessels. (**a**, upper panel) Representative sections after Ki-67 staining at the venous stenosis of the LV-shRNA-*VEGF-A* (LV) and scrambled shRNA (control (C)) or Avastin-treated vessels or immunoglobulin G (IgG) controls at days 14 (D14) and 28 (D28). Nuclei staining brown are positive for Ki-67. IgG antibody staining was performed to serve as negative controls. *Indicates the lumen. All are original magnification ×40. Bar = 200 μm. Pooled data for the LV and C groups or Avastin-treated vessels or IgG controls are shown in the lower panel. This demonstrates a significant decrease in the mean Ki-67 index in the LV-transduced vessels when compared with the C vessels at day 14 ($P<0.01$). Similar results are seen with Avastin-treated vessels when compared with controls at day 14 ($P<0.01$). Significant difference from control value is indicated by $^{**}P<0.001$. Each bar shows mean ± s.e.m. of four animals per group. Pooled data for real-time PCR (RT-PCR) analysis of (**b**) *MMP-2* and (**c**) *MMP-9* expression after transduction with either LV or C are shown. This demonstrates a significant reduction in the average amount of (**b**) *MMP-2* and (**c**) *MMP-9* in the LV-transduced vessels when compared with C vessels at day 7 ($P<0.0001$) with a significant increase in *MMP-2* by day 28 ($P<0.01$). Significant difference from control value is indicated by $^{*}P<0.01$ and $^{\#}P<0.0001$. (**b**, **c**) Each bar shows mean ± s.e.m. of four animals per group. A representative zymogram for (**d**) *MMP-2* and (**e**) *MMP-9* is shown in the upper panel and the pooled data in the lower panels. By zymography, (**d**) *pro-MMP-2* expression was significantly decreased in the LV-transduced vessels when compared with C vessels at day 7 ($P<0.0001$), and by day 14 both pro and active *MMP-2* were significantly decreased (both $P<0.0001$). By zymography, (**e**) *active-MMP-9* expression was significantly decreased in the LV-transduced vessels when compared with C vessels at day 14 ($P<0.001$). (**d**, **e**) Each bar shows mean ± s.e.m. of 3–6 animals per group. Two-way analysis of variance (ANOVA) followed by Student's *t*-test with *post hoc* Bonferroni's correction was performed. Significant difference from control value is indicated by $^{*}P<0.01$, $^{**}P<0.001$, or $^{\#}P<0.0001$.

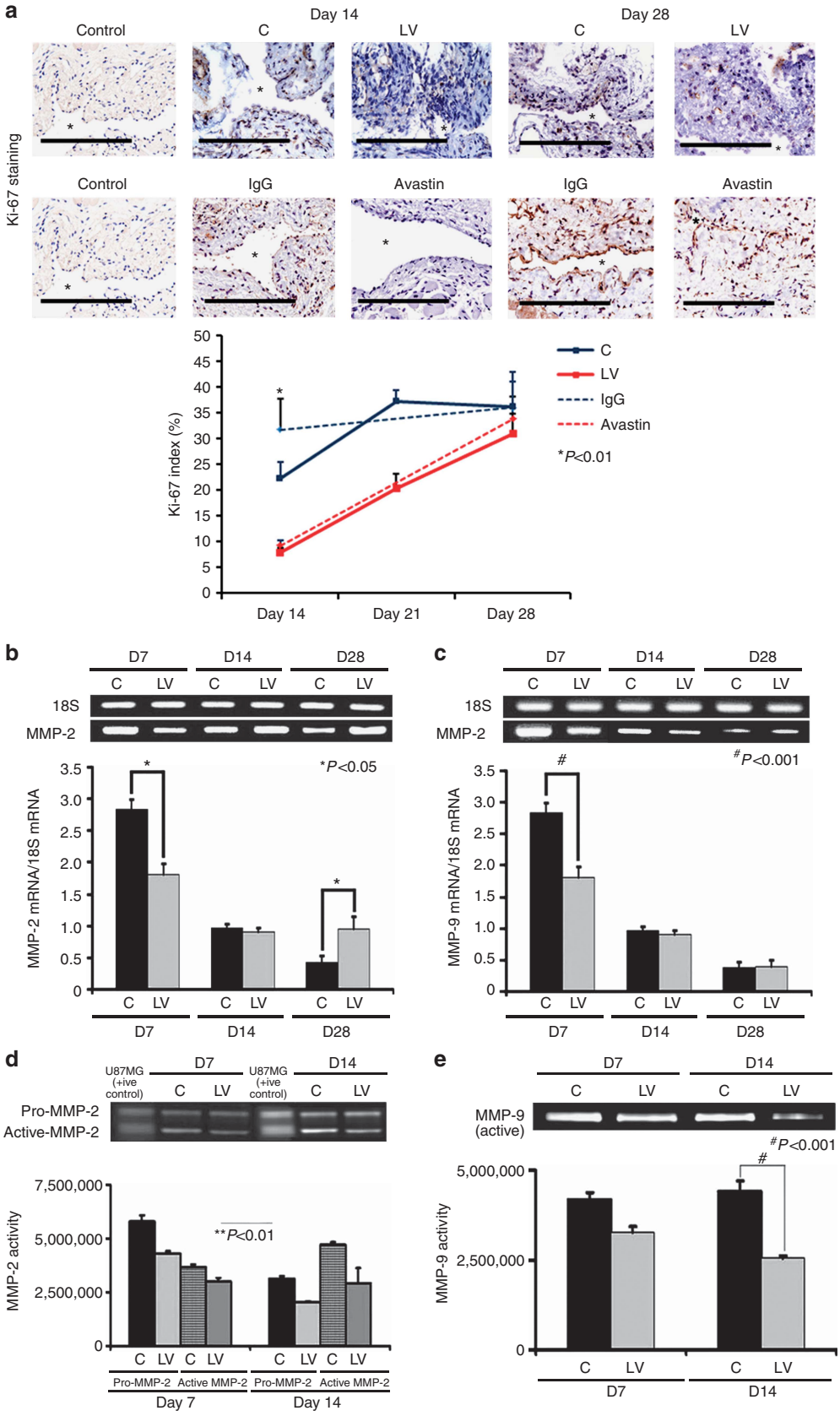
a
Day 14
Day 28
Control
C
LV
C
LV
Ki-67 staining
Control
IgG
Avastin
IgG
Avastin
Ki-67 index (%)
C
LV
IgG
Avastin
*P<0.01
Day 14
Day 21
Day 28
b
D7
D14
D28
C
LV
18S
MMP-2
*P<0.05
MMP-2 mRNA/18S mRNA
c
*P<0.001
MMP-9 mRNA/18S mRNA
d
U87MG (+ive control)
Pro-MMP-2
Active-MMP-2
**P<0.01
MMP-2 activity
Pro-MMP-2
Active MMP-2
Day 7
Day 14
e
MMP-9 (active)
*P<0.001
MMP-9 activity

Table 1 | Synopsis of major findings

	Day 7	Day 14	Day 21	Day 28
VEGF-A	↓	NC		NC
LVA		↑	↑	↑
CD31		↓	↓	↓
Sirius red	↓	↓	↓	NC
TUNEL		↑	NC	NC
Caspase 3	↑	↑		
Ki-67		↓	↓	NC
RT-PCR				
MMP-2	↓	NC		↑
Pro-MMP-2	↓	↓		
Active-MMP-2	NC	↓		
RT-PCR				
MMP-9	↓	NC		NC
MMP-9	NC	↓		
α-SMA		NC	↓	↓
VEGFR-1	↓	NC		NC
HIF-1α	NC	↓		
VEGF-A staining	↓	↓		

Abbreviations: HIF-1α, hypoxia-inducible factor-1α; LVA, lumen vessel area; *MMP-2*, matrix metalloproteinase 2; *MMP-9*, matrix metalloproteinase 9; NC, no change; RT-PCR, real-time PCR; α-SMA, α-smooth muscle actin; TUNEL, TdT-mediated dNTP nick end labeling; *VEGF-A*, vascular endothelial growth factor-A; *VEGFR-1*, vascular endothelial growth factor receptor 1.
NC is no change between the lentivirus (LV)–small hairpin RNA (shRNA)–*VEGF-A*-transduced specimens and controls.
The symbol '↑' indicates significant increase between the LV-shRNA-*VEGF-A*-transduced specimens and controls.
The symbol '↓' indicates significant decrease between the LV-shRNA-*VEGF-A*-transduced specimens and controls.

Avastin-treated vessels, when compared with controls, there was a trend to a significant decrease in the average area of the media and adventitia by day 28 ($P<0.001$, average decrease: 89%). Interestingly, we did not observe a difference in the average area of the neointima of either treatment (lentiviral *VEGF-A* or Avastin) at any time point, suggesting that the positive remodeling may be related to the favorable adventitial and medial remodeling, possibly because of a decrease in the migration of fibroblasts and smooth muscle cells.

We next determined whether the increase in positive vascular remodeling was due to a decrease in the collagen 1 and 3 content using picrosirius staining. Yellow color is positive for collagen 1 or 3 staining (Figure 2a and Supplementary Figure S2 online). As shown, picrosirius staining was decreased at days 3, 7, 14, and 21, with recovery by day 28. We also observed at days 3 and 7 that there was a reduction of the collagen expression in the adventitia and media with expression of collagen localized in the intimal area, which persisted at days 14 and 21 (Supplementary Figure S2 online).

Patency of the LV-shRNA-*VEGF-A* and control shRNA–transfected vessels at days 3, 7, 14, and 28

Patency of the fistula was determined visually by occluding the outflow vein before harvesting the tissue. In a patent fistula, occluding the outflow vein would allow the fistula to dilate, whereas an occluded fistula would not dilate. This was performed several times to be certain that the fistula was occluded or patent. A Kaplan–Meier estimate was performed for the LV-shRNA-*VEGF-A*-transduced vessels compared with controls, as shown in Figure 2d. This showed a significant difference in the patency between the LV-shRNA-*VEGF-A*-transduced vessels when compared with controls (Log-rank test: $P<0.05$).

Adventitial transduction of LV-shRNA-*VEGF-A* to the outflow vein increases apoptosis at day 14

Current literature suggests that *VEGF-A* is needed for maintaining cellular homeostasis, and therefore we hypothesized that decreasing *VEGF-A* would result in increased apoptosis.[25] Apoptosis was first assessed using TUNEL (TdT-mediated dNTP nick end labeling) staining performed on sections removed after transduction with either LV-shRNA-*VEGF-A* or control shRNA (Figure 3, upper panel). By day 14, the average TUNEL index (number of TUNEL-positive cells (brown)/total number of cells×100) at the outflow vein of the LV-shRNA-*VEGF-A* group was significantly higher than the control group (40.4 ± 1.4 vs. 20.6 ± 2.9, respectively, average increase: 196%, $P<0.0001$, Figure 3, lower panel), with no significant differences by days 21 and 28. Similar observations were made in the Avastin-treated vessels when compared with controls. By day 14, there was a significant increase in the TUNEL index in the Avastin-treated vessels when compared with controls (3.8 ± 0.5 vs. 16.8 ± 1.8, respectively, average increase: 442%, $P<0.0001$, Figure 3, lower panel).

Caspase 3 is an effector of apoptosis. We hypothesized that increased caspase 3 activity would be present in sections removed from the outflow vein after transduction with either LV-shRNA-*VEGF-A* or control shRNA. By days 3–14, the average caspase 3 activity was significantly higher in the LV-shRNA-*VEGF-A*-transduced vessels when compared with controls (average increase: 281% at day 3, 368% at day 7, and 365% at day 14, all $P<0.001$, Figure 3b). Overall, these results indicate that adventitial delivery of LV-shRNA-*VEGF-A* results in a significant increase in caspase 3 activity with accompanying increased TUNEL index at the outflow vein, suggesting that there is increased cell death in LV-shRNA-*VEGF-A*-transduced vessels when compared with controls (Table 1). Similar findings were observed in Avastin-treated vessels when compared with controls.

Adventitial transduction of LV-shRNA-*VEGF-A* to the outflow vein decreases cellular proliferation

VEGF-A is needed for cells to proliferate, and we determined cell proliferation by performing Ki-67 staining on sections from the outflow vein after transduction with either LV-shRNA-*VEGF-A* or control shRNA (Figure 4a, upper panel). The average Ki-67 index (number of Ki-67-positive cells (brown)/total number of cells×100) in the LV-shRNA-*VEGF-A* group was significantly lower than the control group by day 14 (7.9 ± 1 vs. 24.6 ± 2.9, respectively, average reduction: 68%, $P<0.01$, Figure 4a, lower panel) and by day 21 (25.5 ± 1.3 vs. 37.2 ± 2.3, respectively, average reduction: 35%, $P<0.01$). In the Avastin-treated vessels when compared with controls, similar findings were observed at day 14 (9.6 ± 0.8 vs. 31.7 ± 6.1, respectively, average reduction: 70%,

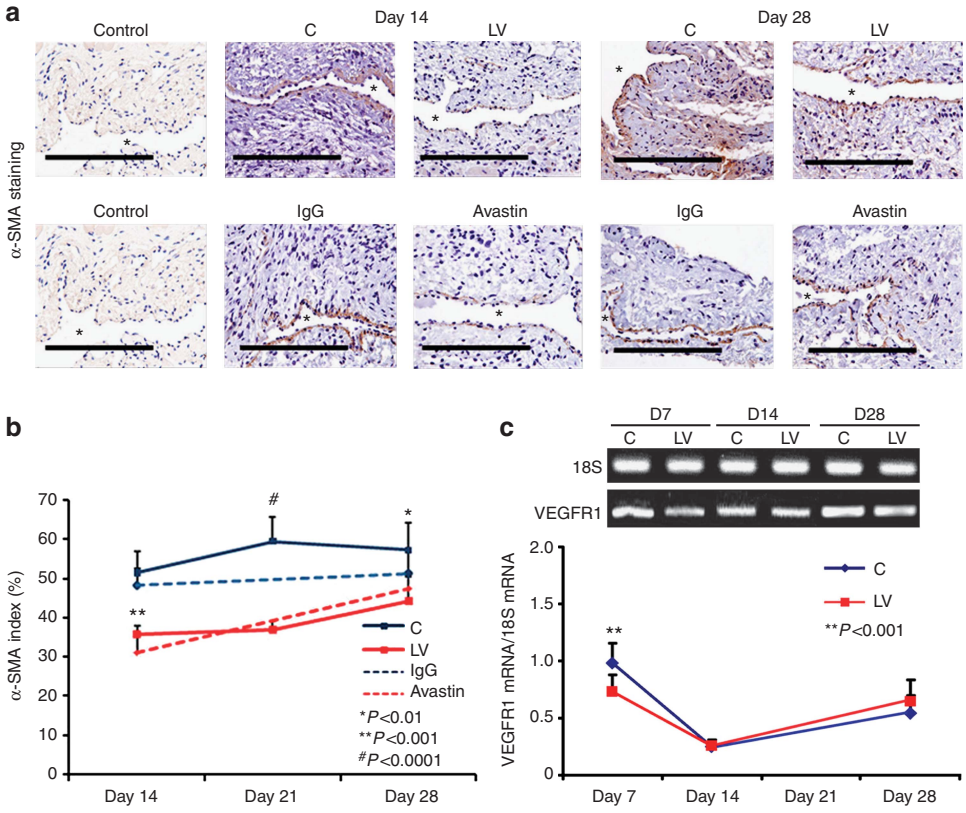

Figure 5 | Smooth muscle cell index and vascular endothelial growth factor receptor 1 (*VEGFR-1*) expression are reduced in lentivirus (LV)–small hairpin RNA (shRNA)–vascular endothelial growth factor-A (*VEGF-A*)–transduced vessels. (**a**, upper panel) Representative sections after α-smooth muscle actin (α-SMA) staining at the venous stenosis of the LV-shRNA-*VEGF-A* (LV) and scrambled shRNA (control (C)) and Avastin treated with control vessels at days 14 and 28. Cells staining brown are positive for α-SMA. immunoglobulin G (IgG) antibody staining was performed to serve as negative control. *Indicates the lumen. All are original magnification ×40. Bar = 200 μm. Pooled data for the LV and C groups and Avastin-treated and control vessels are shown in **a** (lower panel). This demonstrates a significant reduction in the average α-SMA index in LV-transduced vessels when compared with C vessels by day 21 ($P<0.001$) and day 28 ($P<0.01$). There is also a significant decrease in the average α-SMA index in Avastin-treated vessels when compared with controls by day 14 ($P<0.001$). (**c**) Pooled data from RT-PCR analysis for *VEGFR-1* expression after transduction from the LV and C groups. A typical blot is shown in the upper panel and the pooled data in the lower panel (**c**). This demonstrates a significant reduction in the mean *VEGFR-1* expression in the LV-transduced vessels when compared with C vessels at day 7 ($P<0.001$). (**b**, **c**) Each bar shows mean ± s.e.m. of 4–6 animals per group. Two-way analysis of variance (ANOVA) followed by Student's *t*-test with *post hoc* Bonferroni's correction was performed. Significant difference from control value is indicated by $^{*}P<0.01$, $^{**}P<0.001$, or $^{\#}P<0.0001$.

$P<0.01$). In both experimental groups, by day 28, there was no difference between LV-shRNA-*VEGF-A* or Avastin and controls. Overall, these results indicate that cellular proliferation in the scrambled group is increasing with the length of time of fistula and decreasing in the LV-shRNA-*VEGF-A* group with reduction in both LV-shRNA-*VEGF-A*- and Avastin-treated vessels (Table 1).

Adventitial transduction of LV-shRNA-*VEGF-A* to the outflow vein reduces the expression of *MMP-2* and *MMP-9* at the outflow vein

Several studies have shown that there is increased expression of *MMP-2* and *MMP-9* in animal models of hemodialysis AVF and graft failure, as well as in clinical samples.[7,11–14] *MMP-2* and *MMP-9* gene products are thought to be responsible for cellular proliferation and cell migration, resulting in VNH formation.[7,11–14] To test this hypothesis, we designed a set of experiments to ascertain whether reducing *VEGF-A* expression would lead to a reduction in *MMP-2* and *MMP-9* expression.[26] Gene expression of *MMP-2* and *MMP-9* was determined by RT-PCR analysis on specimens removed from the outflow vein transduced with either LV-shRNA-*VEGF-A* or control shRNA. By day 7, the average gene expression of both *MMP-2* and *MMP-9* was significantly lower in the LV-shRNA-*VEGF-A*-transduced vessels when compared with control shRNA (*MMP-2*: 2.04 ± 0.23 vs. 2.87 ± 0.25, respectively, average reduction: 29%, $P<0.0001$, Figure 4b and *MMP-9*: 0.98 ± 0.13 vs. 2.63 ± 0.17, respectively, average reduction: 63%, $P<0.0001$, Figure 4c). By day 14, there was no difference in the mean gene expression of *MMP-2* and *MMP-9* between both groups (P = NS); however, by day 28, there was a significant increase in *MMP-2* expression at the LV-shRNA-transduced vessels when compared with controls (0.96 ± 0.3 vs. 0.39 ± 0.13, respectively, average increase: 246%, $P<0.01$).

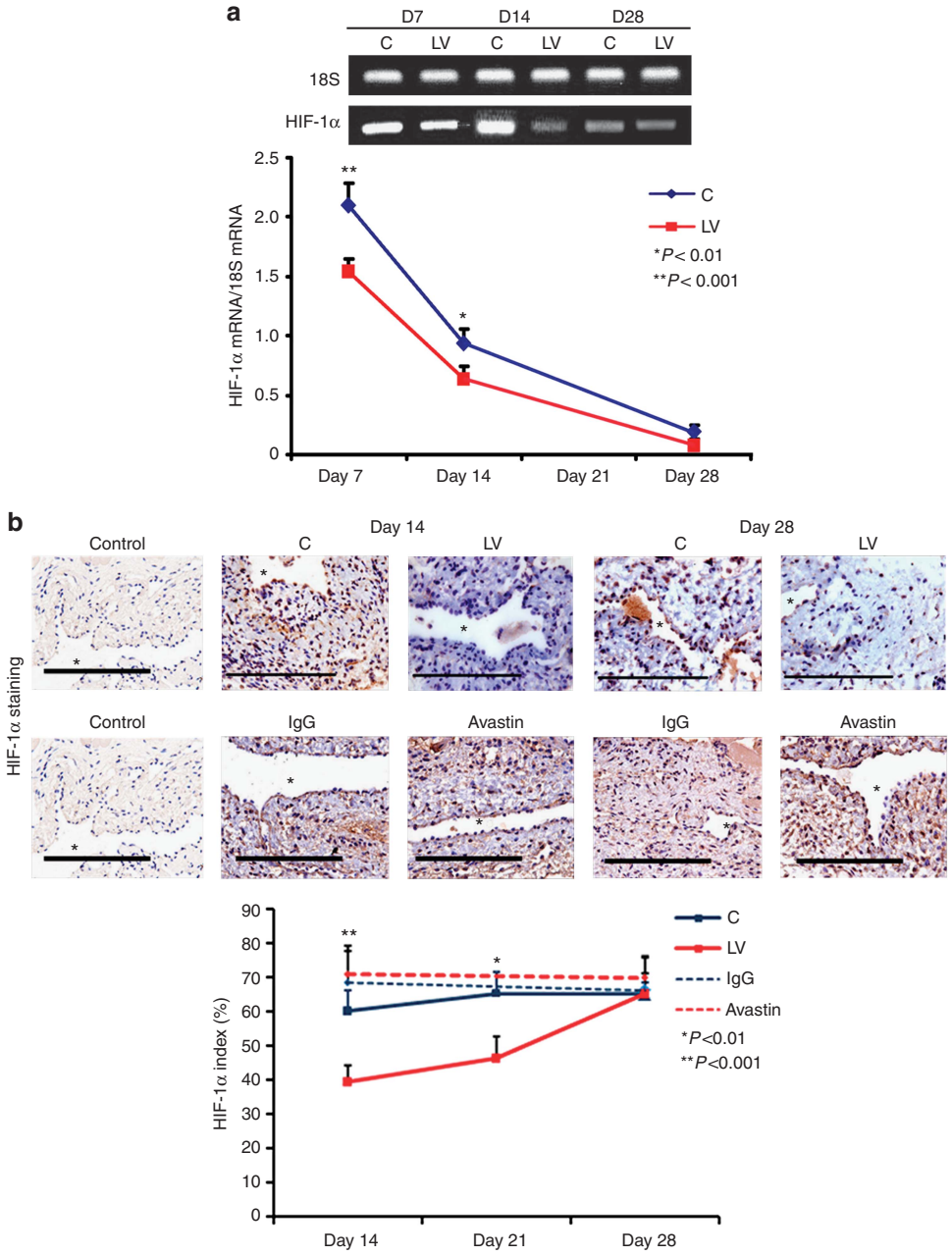

Figure 6 | There is decreased hypoxia-inducible factor-1α (HIF-1α) expression and staining in lentivirus (LV)–small hairpin RNA (shRNA)–vascular endothelial growth factor-A (*VEGF-A*)-transduced and Avastin-treated vessels. (**a**) Real-time PCR (RT- PCR) analysis for HIF-1α expression after transduction with LV and control shRNA (C). A typical blot is shown in the upper panel and the pooled data in the lower panel. This demonstrates a significant reduction in average HIF-1α expression in the LV-transduced vessels when compared with C vessels at days 7 (D7; $P<0.001$) and 14 (D14; $P<0.01$). (**b**) Representative sections after HIF-1α staining at the venous stenosis of the LV-shRNA-*VEGF-A* (LV) and C and Avastin- and immunoglobulin G (IgG)–treated vessels at day 14 and day 28. Brown-staining cells are positive for HIF-1α. IgG antibody staining was performed to serve as negative control. *Indicates the lumen. All are original magnification ×40. Bar = 200 μm. Pooled data for the LV-transduced and C vessels and Avastin-treated and control vessels are shown in **b**. This demonstrates a significant reduction in the average HIF-1α index in the LV-transduced vessels when compared with C vessels at days 14 ($P<0.001$) and 21 ($P<0.01$). There is a significant reduction in the average HIF-1α index in the LV-transduced vessels when compared with C vessels at days 14 ($P<0.001$) and 21 ($P<0.01$). There is no difference in the Avastin-treated vessels compared with controls at either time point. Each bar shows mean ± s.e.m. of 4–6 animals per group. Two-way analysis of variance (ANOVA) followed by Student's *t*-test with *post hoc* Bonferroni's correction was performed. Significant difference from control value is indicated by $^{\#}P<0.001$.

Because the translation of the protein lags behind the gene changes, we assessed the protein activity of *MMP-2* and *MMP-9* using zymography performed on the outflow vein transduced with either LV-shRNA-*VEGF-A* or control shRNA at days 7 and 14. By day 7, the average *pro-MMP-2* activity was significantly lower in the LV-shRNA-*VEGF-A*-transduced vessels when compared with control vessels (4,309,376 ± 150,167 vs. 5,788,726 ± 12,611, respectively,

average reduction: 26%, $P<0.0001$, Figure 4d), and by day 14 both *pro* and *active MMP-2* were significantly lower in the LV-shRNA-*VEGF-A*-treated vessels when compared with controls (*pro-MMP-2*: 3,124,526 ± 122,611 vs. 2,056,144 ± 150,167, respectively, average reduction: 52%, $P<0.0001$, *active MMP-2*: 2,056,149 ± 150,167 vs. 4,309,376 ± 150,168, respectively, average reduction: 52%, $P<0.0001$). By day 14, the average *active MMP-9* activity was significantly lower in the LV-shRNA-*VEGF-A*-transduced vessels when compared with control vessels (2,542,569.5 ± 183,929 vs. 3,424,355 ± 150,178, respectively, average reduction: 26%, $P<0.001$, Figure 4e) (Table 1).

Adventitial transduction of LV-shRNA-*VEGF-A* to the outflow vein decreases α-SMA expression

The majority of the cells comprising VNH are positive for α-SMA. Outflow sections from LV-shRNA-*VEGF-A* and control groups were stained for α-SMA (Figure 5a). The average SMA index (number of SMA-positive cells (brown)/total number of cells×100) at the outflow vein of the LV-shRNA-*VEGF-A*-transduced vessels was significantly lower than the control group by day 21 (36.9 ± 2.3 vs. 63.3 ± 5.8 respectively, average reduction: 42%, $P<0.001$, Figure 5b) and day 28 (39.8 ± 6.9 vs. 65.3 ± 6.9, respectively, average reduction: 37%, $P<0.01$). We performed vimentin staining and observed no difference between the two groups (Supplementary Figure S3 online). By day 14, there was a significant reduction in the SMA index in the Avastin-treated vessels when compared with controls (32.8 ± 2.1 vs. 53.1 ± 4.1 respectively, average reduction: 38%, $P<0.001$).

Smooth muscle cells express *VEGFR-1*. Smooth muscle cell expression was performed using RT-PCR analysis for *VEGFR-1*. The mean gene expression for *VEGFR-1* by day 7 at the LV-shRNA-*VEGF-A*-transduced vessels was significantly lower than the control group (0.69 ± 0.06 vs. 1.03 ± 0.06, respectively, average reduction: 34%, $P<0.001$, Figure 5c). By days 14 and 28, there was no difference between the two groups ($P=$NS).

VEGF-A silencing is associated with decreased mRNA levels and immunostaining for HIF-1α

Because increased expression of HIF-1α has been observed in animal models of hemodialysis graft failure and in clinical specimens from patients with chronic graft failure, we determined the expression levels for HIF-1α in outflow vein sections transduced with either LV-shRNA-*VEGF-A* or control shRNA. The mean gene expression of HIF-1α (Figure 6a) at the LV-shRNA-*VEGF-A*-transduced vessels was significantly lower than the control vessels by day 7 (1.54 ± 0.11 vs. 2.1 ± 0.17, respectively, average reduction: 27%, $P<0.001$) and day 14 (0.64 ± 0.1 vs. 1.04 ± 0.06, respectively, average reduction: 39%, $P<0.01$).

We next determined the expression of HIF-1α by immunostaining (Figure 6b). The average HIF-1α index (number of HIF-1α-positive cells (brown)/total number of cells×100) of LV-shRNA-*VEGF-A*-transduced vessels when compared with controls at day 14 (35.3 ± 3.4 vs. 63.1 ± 6.6, respectively, average reduction: 44%, $P<0.001$, Figure 6b) and day 21 (52.9 ± 2.5 vs. 74.2 ± 4.5, respectively, average reduction: 29%, $P<0.01$). There was no difference by day 28 in the LV-shRNA-*VEGF-A*-transduced vessels when compared with controls. In the Avastin-treated vessels, when compared with controls, there was no difference in the HIF-1α index at day 14 or day 28.

VEGF-A silencing in hypoxic fibroblasts reduces α-SMA production at 24 and 72 h

Previous studies have demonstrated that HIF-1α gene expression is increased in failed hemodialysis graft specimens removed from patients and in animal models of graft failure, and other studies indicate that hypoxia can cause an increase in fibroblast to myofibroblast differentiation.[11,24,27–29] To investigate this possibility, we determined whether reducing *VEGF-A* gene expression in fibroblasts and then subjecting them to hypoxia would cause a decrease in α-SMA production. Murine AKR-2B cells transduced with either LV-shRNA-*VEGF-A* (LV) or control shRNA-*VEGF-A* (C) were subjected to 24 or 72 h of hypoxia. Expression of α-SMA in the cell lysate was determined using western blot analysis. Our results indicate a significant reduction in α-SMA production at 24 h (17.7 ± 1.5 vs. 45.9 ± 4.6, LV-shRNA-*VEGF-A* vs. control shRNA, respectively, average reduction: 61%, $P<0.0001$) and 72 h (17 ± 3 vs. 66.3 ± 9.2, LV-shRNA-*VEGF-A* vs. control shRNA, respectively, average reduction: 74%, $P<0.0001$) of hypoxia when compared with controls (Figure 7a). Confocal microscopy for α-SMA staining performed on AKR-2B cells transduced with either LV-shRNA-*VEGF-A* or control shRNA that had been subjected to 24 or 72 h of hypoxia demonstrated similar results (Figure 7b). Semiquantitative analysis for cells staining positive for α-SMA (red) demonstrated a significant decrease in the intensity of the α-SMA staining in the LV-shRNA-*VEGF-A*-transduced cells when compared with controls at 24 h (132 ± 5.8 vs. 179 ± 3.4, respectively, average reduction: 27%, $P<0.0001$) and 72 h (18.7 ± 9.42 vs. 100 ± 9.5, respectively, average reduction: 71%, $P<0.0001$, Figure 7c).

VEGF-A silencing in hypoxic fibroblasts reduces proliferation and invasion

We next determined whether reducing *VEGF-A* gene expression in fibroblasts and subsequently subjecting them to hypoxia would decrease the proliferative potential (thymidine incorporation assay) of fibroblasts when compared with controls. Murine AKR-2B cells transduced with either LV-shRNA-*VEGF-A* or control shRNA were subjected to normoxia and hypoxia, and proliferation assay was performed. This demonstrated a significant reduction in LV-shRNA-*VEGF-A*-transduced cells when compared with controls for normoxia at 48 h (85,552 ± 5428 vs. 50,498 ± 3346, control shRNA vs. LV-shRNA-*VEGF-A*, respectively, average reduction: 41%, $P<0.05$, Figure 7d), with significant reduction in hypoxia at 48 h (75,658 ± 2915 vs. 50,243 ± 1851, control shRNA vs. LV-shRNA-*VEGF-A*,

respectively, average reduction: 34%, $P<0.0001$) and 72 h (110,250 ± 1843 vs. 85,895 ± 1492, control shRNA vs. LV-shRNA-*VEGF-A*, respectively, average reduction: 22%, $P<0.0001$).

As the proliferative ability of these cells was reduced, we determined whether the invasive capacity of these cells was reduced under the same conditions. Murine AKR-2B cells transduced with either LV-shRNA-*VEGF-A* or control shRNA

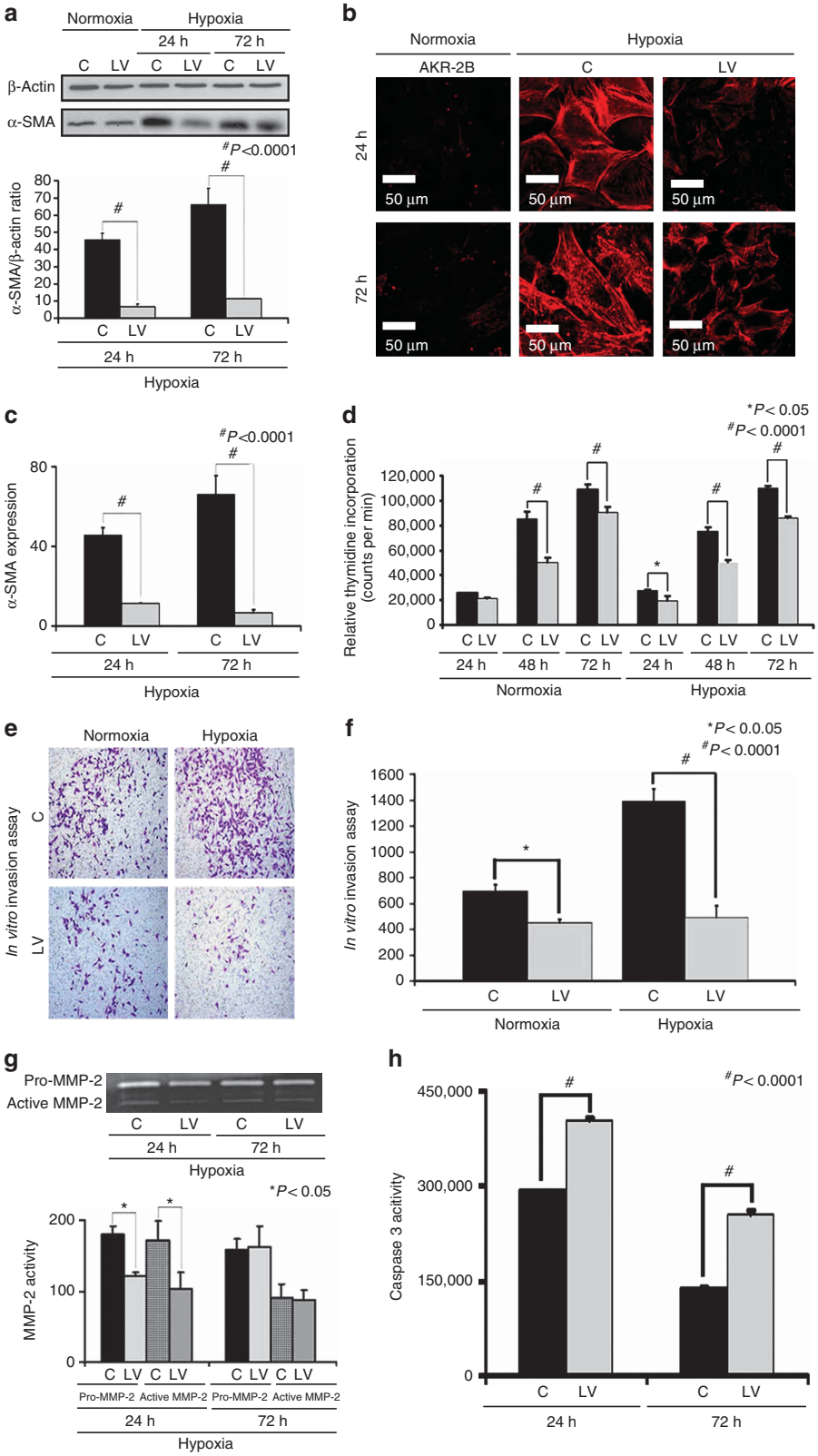

were subjected to normoxia and hypoxia, and a matrigel invasion assay was performed. This demonstrated a significant reduction in the invasive potential of LV-shRNA-*VEGF-A*-transduced cells when compared with control (normoxia: 600 ± 10 vs. 400 ± 10, control shRNA vs. LV-shRNA-*VEGF-A*, respectively, average reduction: 33%, $P < 0.05$; hypoxia: 1400 ± 10 vs. 400 ± 10, control shRNA vs. LV-shRNA-*VEGF-A*, respectively, average decrease: 350%, $P < 0.0001$, Figure 7e and f).

VEGF-A silencing in hypoxic fibroblasts decreases *MMP-2* activity and increases caspase 3 activity

Because there was a decrease in proliferation and invasion in cells transduced with LV-shRNA-*VEGF-A*, we determined whether there was a decrease in *MMP-2* expression using zymography. We observed a significant decrease in the *pro MMP-2* (122 ± 5.4 vs. 180 ± 11, LV-shRNA-*VEGF-A* vs. control shRNA, respectively, average reduction: 33%, $P < 0.05$) and active *MMP-2* activity (103 ± 24 vs. 171 ± 28, LV-shRNA-*VEGF-A* vs. control shRNA, respectively, average reduction: 33%, $P < 0.05$) at 24 h, with no difference by 72 h ($P =$ NS, Figure 7g).

As *VEGF-A* is involved in cellular homeostasis, we determined whether reducing *VEGF-A* expression would result in an increase in caspase 3 activity (Figure 7h). We observed a significant increase in caspase 3 activity in LV-shRNA-*VEGF-A*-transduced cells when compared with controls at 24 h ($405{,}725 \pm 1013$ vs. $292{,}723 \pm 558$, respectively, average increase: 160%, $P < 0.0001$) and 72 h ($254{,}277 \pm 5870$ vs. $137{,}980 \pm 2810$, respectively, average increase: 184%, $P < 0.0001$) of hypoxia.

DISCUSSION

It is estimated that the number of patients with end-stage renal disease who use hemodialysis as the preferred mode of therapy will double in the next decade.[1] For patients to receive adequate hemodialysis, a well-functioning vascular access is needed. The 'Achilles heel' of hemodialysis AVF or grafts is stenosis formation caused by VNH that typically occurs in the proximal outflow vein.[6] Recent studies have shown that 1-year primary patency of an AVF is 61% and that the 6-month patency rates after angioplasty of venous stenosis range from 0 to 23%.[30,31] The mechanisms underlying the formation of VNH associated with hemodialysis AVF or graft failure remain poorly understood.

VEGF-A is a multifunctional cytokine that has been shown to be involved in cell proliferation, migration, and cell death.[25] Previous studies from our laboratory using experimental animal models of VNH formation in hemodialysis AVF or graft failure have demonstrated that there is increased expression of *VEGF-A* and *VEGFR-1* at the venous stenosis when compared with the control vein ($P < 0.05$).[11–13] Increased expression of *VEGF-A* has been localized to the adventitia and neointima in samples removed from patients with failed hemodialysis vascular access.[6] A recent study from our laboratory demonstrated that simvastatin treatment before the placement of AVF in a murine model of chronic kidney disease reduced VNH formation by decreasing *VEGF-A* and *MMP-9* expression.[10] In this study, we targeted the adventitia using LV-shRNA-*VEGF-A* to reduce *VEGF-A* gene expression, which resulted in a significant increase in luminal vessel area, significant decrease in the media/adventitia area, and a decrease in collagen expression. We further observed similar results when we used systemic delivery of Avastin. In both forms of therapy, a significant reduction in *VEGF-A* staining was observed as well.

The result of silencing *VEGF-A* had two very important effects. First, *VEGF-A* is needed for cell survival, and in this study the decrease in *VEGF-A* resulted in increased cell death, as demonstrated by increased caspase 3 activity and TUNEL staining. Furthermore, we observed a decrease in cells staining positive for α-SMA with a decrease in *VEGFR-1* expression. *VEGFR-1* is needed for cell proliferation and migration, and a recent study showed that it might influence cell death of smooth muscle cells.[16] These results are consistent with reports in animal models of arterial stenosis that showed that blockade of *VEGF-A* using soluble *VEGFR-1* reduces intimal hyperplasia by blocking

Figure 7 | There is decreased proliferation, invasion, α-smooth muscle actin (α-SMA), and matrix metalloproteinase 2 (*MMP-2*) expression with increased caspase 3 activities in the lentivirus (LV)–small hairpin RNA (shRNA)–vascular endothelial growth factor-A (*VEGF-A*)–transduced cells subjected to hypoxia. Western blot for α-SMA after transduction LV-shRNA-*VEGF-A* (LV) and scrambled shRNA-*VEGF-A* (C) in AKR-2B fibroblasts subjected to hypoxia at 24 and 72 h. A typical western blot is shown in the upper panel and the pooled data in the lower panel (**a**). This demonstrates a significant reduction in the mean α-SMA expression in the LV-transduced cells when compared with C cells at 24 ($P < 0.0001$) and 72 h ($P < 0.0001$). (**b**) Staining for α-SMA (red positive cells) at 24 and 72 h. (**c**) Pooled data for the average intensity of cells staining positive for α-SMA, demonstrating a significant decrease in the LV-transduced cells when compared with C cells at both 24 and 72 h (both $P < 0.001$). (**d**) Pooled data for proliferation using the thymidine incorporation assay for the LV-transduced cells when compared with C cells, showing a significant decrease in proliferation for the normoxic groups at 48 and 72 h ($P < 0.0001$) and for 24 ($P < 0.05$), 48, and 72 h ($P < 0.0001$) of hypoxia. (**e**) Invasion assay for LV-transduced cells when compared with C cells for normoxia and hypoxia. (**f**) Pooled data for invasion of the LV-transduced cells when compared with C cells, showing a significant decrease in both the normoxic ($P < 0.0001$) and hypoxic groups ($P < 0.0001$). (**g**) Upper panel is a representative zymogram of LV-transduced cells when compared with C cells subjected to hypoxia at 24 and 72 h, and the lower panel shows pooled data demonstrating a significant reduction in both *pro-* and *active-MMP-2* activity at 24 h for LV-transduced cells when compared with C cells ($P < 0.05$). (**h**) Pooled caspase 3 activity in LV-transduced cells when compared with C cells subjected to hypoxia at 24 and 72 h, showing a significant increase in the mean caspase 3 activity in the LV-transduced cells when compared with C cells at 24 and 72 h (both $P < 0.0001$). (**c**) Each bar shows mean ± s.e.m. of 3–6 different experiments per group. Two-way analysis of variance (ANOVA) followed by Student's *t*-test with *post hoc* Bonferroni's correction was performed. Significant difference from control value is indicated by $^{*}P < 0.05$, $^{**}P < 0.01$, or $^{\#}P < 0.001$.

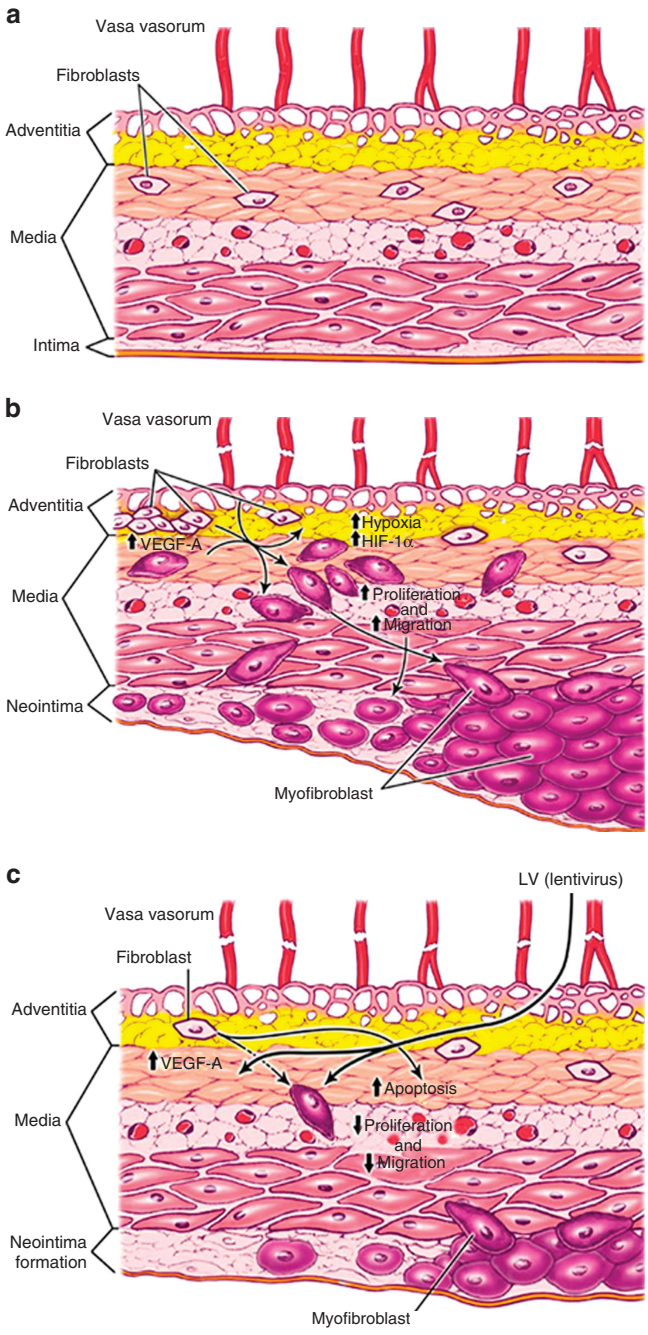

Figure 8 | Cartoon of proposed mechanism. Schematic showing (**a**) normal vein, (**b**) vein after arteriovenous fistula (AVF) placement, and (**c**) outflow vein after fistula placement with lentivirus (LV)–small hairpin RNA (shRNA)–vascular endothelial growth factor-A (*VEGF-A*) silencing and its different mechanisms. HIF-1α, hypoxia-inducible factor-1α.

recruitment of monocytes.[21,22] In contrast, increased expression of *VEGFR-1* has been associated with increased proliferation of mesenchymal cells such as vascular smooth muscle and allied synthetic phenotypes.[19]

The second important effect of reducing mRNA for *VEGF-A* was a decrease in cellular proliferation and reduction of Ki-67 staining in both LV-shRNA-*VEGF-A*-transduced and Avastin-treated vessels when compared with controls. This

Table 2 | PCR primers used in this study

Gene	Sequence	Amplicon length	Cycles
HIF-1α	5′-AGTGATGAAAGAATTACT-3′ (sense) 5′-AATAATACCACTTACAACA-3′ (antisense)	2759	35
VEGF-A	5′-ATGAAGTGATCAAGTTCATGG-3′ (sense) 5′-GGATCTTGGACAAACAAATGC-3′ (antisense)	360	35
VEGFR-1	5′-TTTCCATTTGATACTCTTAC-3′ (sense) 5′-TCTTAGTTGCTTTACCAGGG-3′ (antisense)	310	35
MMP-2	5′-AGATCTTCTTCTTCAAGGACCGGTT-3′ (sense) 5′-GGCTGGTCAGTGGCTTGGGGTA-3′ (antisense)	225	35
MMP-9	5′-GTTTTTGATGCTATTGCTGAGATCCA-3′ (sense) 5′-CCCACATTTGACGTCCAGAGAAGAA-3′ (antisense)	208	35
18S	5′-AGCTAGGAATAATGGAATAG-3′ (sense) 5′-AATCAAGAACGAAAGTCGGAG-3′ (antisense)	150	

Abbreviations: *HIF-1α*, hypoxia-inducible factor-1α; *MMP-2*, matrix metalloproteinase 2; *MMP-9*, matrix metalloproteinase 9; *VEGF-A*, vascular endothelial growth factor-A; *VEGFR-1*, vascular endothelial growth factor receptor 1.

reduction in cellular proliferation was associated with a reduction of several important genes responsible for cellular migration including *MMP-2* and *MMP-9*. In patients with failed vascular access, as well as in experimental animal models of hemodialysis AVF or graft failure, increased expression of *MMP-2* with adventitial localization of *MMP-2* at the venous stenosis formation has been observed.[11–13] These results are consistent with other studies that have shown *MMP* inhibition in a rat and porcine model of arteriovenous hemodialysis graft failure model has been shown to reduce VNH formation.[32,33]

Adventitial delivery of LV-shRNA-*VEGF-A* demonstrated a 'top-down' effect by showing that silencing mRNA expression for *VEGF-A* was localized to the adventitia and media at day 3 and the whole vessel wall by day 7 after transduction. The temporal and spatial localization of silencing *VEGF-A* corresponds with previous studies that have demonstrated that adventitial fibroblasts and medial cells can contribute to VNH formation.[7–9] In addition, adventitial remodeling has been observed to occur in stenosis associated with arterial injury and lately and that associated with hemodialysis graft failure.[7–9] We observed a significant reduction in the average area of the media and adventitia. Taken collectively, these findings lead us to believe that adventitial and medial remodeling is an important contributor to the positive vascular remodeling that was observed.

Hypoxic injury is known to accelerate conversion of fibroblast to myofibroblasts (α-SMA-positive cells), and increased HIF-1α has been observed in animal models and in clinical specimens of AVF or graft failure.[11,24,27–29] *VEGF-A*-mediated activation of fibroblasts to myofibroblast phenotype is often accompanied by the activation of matrix regulatory signaling moieties including *MMP-2* and

MMP-9.[34] Fibroblasts transduced with either LV-shRNA-*VEGF-A* and subjected to hypoxia had a significant decrease in α-SMA production, decreased invasion, proliferation, *MMP-2* activity, and an increase in caspase 3, offering a potential cellular target for the *in vivo* observations. We demonstrated that mRNA for HIF-1α in the outflow vein vessels of the LV-shRNA-*VEGF-A*-transduced vessels was significantly lower than control vessels, which was confirmed with HIF-1α staining. In Avastin-treated vessels, we observed no difference in HIF-1α index at either time point.

In vivo, we observed a significant reduction in both mRNA and staining for HIF-1α in LV-shRNA-*VEGF-A*-transduced vessels when compared with controls. We speculate that the paradoxical reduction in HIF-1α associated with inhibition of *VEGF* may be related to the decrease in metabolic demand for oxygen secondary to a reduction in proliferation, migration, and cell death. Taken together, these results suggest that anti-*VEGF-A* therapy at the time of fistula placement results in positive vascular remodeling in AVFs because of multiple mechanisms that were mentioned.

Previous experimental models to study hemodialysis AVF or graft failure have used animals with normal kidney function. A recent study demonstrated that animal models with abnormal kidney function have increased VNH formation when compared with animals with normal kidney function.[35] Furthermore, increased expression of *VEGF-A*, *MMPs*, and other important proteins has been found to be elevated in patients on hemodialysis and therefore would be consistent with the data obtained in our animal model.[36–38]

One limitation of this study is that cells such as lymphocytes and macrophages may also have been transduced with LV-shRNA-*VEGF-A* and may also be contributing in part to the observed effects of positive vascular remodeling besides the fibroblast. Another limitation is the choice of mouse strain used to perform the remnant kidney model. It is well known that C57BL/6 mice are resistant to glomerulosclerosis, whereas other animals such as the BALB/c are more prone.[39,40] These genetic differences may influence the outcomes observed in this study. The fistulas were placed in central veins, and these fistulas may behave differently than those placed in peripheral veins. We used Avastin, which is a humanized antibody to *VEGF-A*, and there are reports that it may weakly inhibit murine *VEGF-A*.[41]

In conclusion, our central hypothesis is that VNH formation occurs in part because of local vessel hypoxia caused by surgical trauma to the vasa vasorum supplying the outflow vein at the time of AVF placement (Supplementary Figure S4 online). This hypoxia in turn leads to an increase in gene expression of *VEGF-A*, *MMP-2*, and *MMP-9*, resulting in the activation of adventitial fibroblasts that undergo conversion to myofibroblasts with increased proliferative and migratory capacity, thereby resulting in VNH formation[3,7,11,19,26] (Figure 8b). The normal vein is shown for comparison in Figure 8a. This study demonstrates that adventitial delivery of LV-shRNA-*VEGF-A* decreases the expression of several important promigratory cytokines such as *VEGFR-1*, *MMP-2*, and *MMP-9* (Figure 8c). The net result is an overall decrease in cell proliferation, decrease in α-SMA-positive cells, with increased apoptosis resulting in positive vascular remodeling, decreased media/adventitia area with decreased constrictive remodeling. However, a significant decrease in the average area of the neointima was not observed. The results of these findings were extended to Avastin, which demonstrated similar findings. The clinical significance of this study is that it provides rationale for using anti-*VEGF-A* therapies at the time of fistula creation to reduce VNH formation.

MATERIALS AND METHODS

Experimental animals

Appropriate Institutional Animal Care and Use Committee approval was obtained before performing any procedures. The housing and handling of the animals was performed in accordance with the Public Health Service Policy on Humane Care and Use of Laboratory Animals revised in 2000.[42] Animals were housed at 22 °C temperature, 41% relative humidity, and 12-/12-h light/dark cycles. Animals were allowed access to water and food *ad libitum*. Anesthesia was achieved with intraperitoneal injection of a mixture of ketamine hydrochloride (0.20 mg/g) and xylazine (0.02 mg/g) and maintained with intraperitoneal pentobarbital (20–40 mg/kg). A total of 204 male C57BL/6 mice (Jackson Laboratories, Bar Harbor, ME) weighing 25–30 g were used for this study as depicted. One normal kidney function mouse was used for micro-computed tomography analysis. Chronic renal insufficiency was created by surgical removal of the right kidney accompanied by ligation of the arterial blood supply to the upper pole of the left kidney, as described previously.[14] At 4 weeks after nephrectomy, connecting the right carotid artery to the ipsilateral jugular vein created an AVF.[14,23] Five million PFUs of either LV-shRNA-*VEGF-A* or scrambled-shRNA-*VEGF-A* (control shRNA, nontargeting empty vector) in 5 μl of PBS were injected using a 30-guage needle into the adventitia of the proximal outflow vein at the time of AVF creation at the time of fistula creation.[43] In this animal model, venous stenosis forms reproducibly at this location. Animals were killed at days 3, 7, 14, 21, and 28 following AV fistula placement. RT-PCR, protein, and histologic analyses were obtained. Serum BUN and creatinine were measured by removing blood from the tail vein at baseline (before nephrectomy), at AVF creation, and at the time of killing. In a separate group of animals, intraperitoneal Avastin (5 mg/kg) or isotype-matched IgG was given every other day 1 week before fistula placement and continued up to the time of killing at either day 14 or day 28. Specimens were removed for histomorphometric analysis only.

Vector constructs

The shRNA for *VEGF-A* was obtained from Open Biosystems (Huntsville, AL; (www.openbiosystems.com, RMM4534-NM_001025250), and the lentivirus was prepared according to the manufacturer's protocol.

Tissue harvesting

At the time of killing, all mice were anesthetized as described previously, and the fistula was dissected free of the surrounding tissue. Animals were killed by CO_2 asphyxiation, and the outflow

veins were harvested for RT-PCR, histologic, or protein analyses. For histologic analysis, all vessels were perfusion-fixed before removal.

Cell culture
To determine the efficacy and efficiency of lentiviral silencing on *VEGF-A* expression, murine fibroblast (AKR-2B) cells were transduced with either LV-shRNA-*VEGF-A* or scrambled-shRNA-*VEGF-A*, and the expression was analyzed using RT-PCR or western blotting, as described previously.[10]

Hypoxia chamber
AKR-2B transduced with LV-shRNA-*VEGF-A* or control shRNA were made hypoxic for 24 or 72 h, as previously described.[10,27]

RNA isolation
The tissue was stored in RNA-stabilizing reagent (Qiagen, Gaithersburg, MD) as per the manufacturer's guidelines. To isolate the RNA, the specimens were homogenized and total RNA was isolated using the RNeasy mini kit (Qiagen).[14,23]

RT-PCR analysis
Expression for the gene of interest was determined using RT-PCR analysis, as described previously.[23,10] Primers used are shown in Table 2.

In situ hybridization for *VEGF-A*
In situ hybridization for *VEGF-A* was performed as described elsewhere.[44] Briefly, the digoxigenin-labeled complementary RNA probe was made with plasmid pBS-164-*VEGF* (gift from Andreas Nagy, Toronto, Canada) using digoxigenin RNA labeling kit with T7 RNA polymerase for antisense (complementary to *VEGF* mRNA) probe and T3 RNA polymerase for sense (control) probe (Roche Applied Science, Indianapolis, IN). The probe hybridization was performed as per guidelines from Roche Applied Science. The probe hybridization was visualized using anti-digoxigenin-alkaline phosphatase antibody and NBT-BCIP solution as substrate (Roche Applied Science).

Sodium dodecyl sulfate–polyacrylamide gel electrophoresis zymography for *MMP-2* and *MMP-9*
MMP-2 and *MMP-9* protein activities were determined using zymographic analysis. This was performed on homogenates from cultured cells or outflow veins transduced with either LV-shRNA-*VEGF-A* or control shRNA as described previously.[7,13]

Western blot of α-SMA
We assessed the differentiation of fibroblasts to myofibroblasts by performing western blot analysis for α-SMA. The cultured cells were processed for western blot analysis using rabbit polyclonal antibody, as described previously.[13]

Caspase 3 activity
Apoptosis was assessed using enzyme-linked immunosorbent assay for caspase 3. Cellular protein was extracted from cultured cells and mouse tissue, as described previously. The enzymatic activity of caspase 3 was assessed by Caspase Glo assay (G811C, Promega, Madison, WI) as described earlier.[10]

Proliferation assay
A total of 20,000 AKR-2B cells transduced with LV-shRNA-*VEGF-A* or control shRNA were seeded in 24-well plates and cultured for 24, 48, and 72 h in Dulbecco's modified Eagle's medium. After 20, 44, and 68 h, 1 mCi of [3H]-thymidine was added to each well, and 4 h later cells were washed with chilled PBS, fixed with 100% cold methanol, and collected for measurement of trichloroacetic acid–precipitable radioactivity. Experiments were repeated at least three times for each time point.

Invasion and cell migration assay
A total of 5000 AKR-2B cells transduced with LV-shRNA-*VEGF-A* or control shRNA were seeded in 8 μm Transwells (Corning Life Sciences, Tewksbury, MA) that were precoated with low growth factor matrigel in a serum-free medium. The complete medium was supplemented under the Transwell and incubated for 6 h at 37 °C. After 6 h, Transwells were washed with PBS and fixed with paraformaldehyde (4% v/v). Finally, Transwells were stained with bromophenol (0.1%) solution. The cells from the upper well were removed with cotton-tip applicators. The cells from the bottom well were counted for analysis.

Tissue processing and immunohistochemistry
Each outflow vein from each animal was embedded in paraffin lengthwise so that the sections would be orthogonal to the long axis of the vessel, as described previously.[10] Typically, 80–120 4-mm sections were obtained, and the cuff used to make the anastomosis could be visualized. Every 40-μm, 2–4 sections were stained with hematoxylin and eosin, Ki-67, α-SMA, CD31, HIF-1α, and *VEGF-A* were performed on paraffin-embedded sections from the outflow vein after transduction with either LV-shRNA-*VEGF-A* or control shRNA or Avastin with control using the EnVision (DAKO, Carpinteria, CA) method with a heat-induced antigen retrieval step.[7,13] The following antibodies were used: mouse monoclonal antibody Ki-67 (DAKO, 1:400), CD31 (Abcam, Cambridge, MA; 1:400), rabbit polyclonal antibody to mouse for *VEGF-A* (Abcam, 1:600), rabbit polyclonal antibody to mouse for HIF-1α (Novus Biologicals, Littleton, CO, 1:200), or rabbit polyclonal antibody to mouse for α-SMA (Abcam, 1:400). IgG antibody staining was performed to serve as controls.

TUNEL staining
TUNEL staining[10] was performed on paraffin-embedded sections from the outflow vein after transduction with either LV-shRNA-*VEGF-A* or control shRNA or Avastin or control vessels, as specified by the manufacturer (DeadEnd Colorimetric tunnel assay system, G7360, Promega). Negative control is shown where the recombinant terminal deoxynucleotidyl transferase enzyme was omitted.

Picrosirius red staining
Picrosirius red staining was performed on unstained sections from LV-shRNA-*VEGF-A* and scrambled shRNA *VEGF-A* or Avastin-treated or control vessels at different time points, as described previously.[10]

Morphometry and image analysis
Paraffin-embedded sections (4 μm) immunostained for hematoxylin and eosin stains were viewed with an Axioplan 2 Microscope (Zeiss, Oberkochen, Germany) equipped with a Neo-Fluor×20/0.50 objective and digitized to capture a minimum of 3090×3900 pixels

using a Axiocam camera (Zeiss).[7,10,13] Images covering one entire cross-section from each section of the outflow vein transduced with either LV-shRNA-*VEGF-A* or control shRNA or Avastin treated with control vessels were acquired and analyzed using KS 400 Image Analysis software (Zeiss). For morphometric analysis used to quantify the lumen vessel area and wall vessel area, we used 6–10 4-μm paraffin-embedded sections removed from the outflow vein for each animal at each time point. Sections were subsequently viewed with an Axioplan 2 Microscope (Zeiss) equipped with a Neo-Fluor×20/0.50 objective and digitized to capture at least 1030×1300 pixels and cell density determined along with the vessel wall and luminal vessel areas. The area was measured by tracing the vessel wall using an automated program.[13] Ki-67-positive (brown), α-SMA-positive (brown), TUNEL-positive (brown), HIF-1α-positive (brown), or *in situ* hybridization–positive (brown) cells were highlighted, in turn, by selecting the appropriate red–green–blue color intensity range and then counted. The Ki67, α-SMA, TUNEL, and HIF-1α indices were calculated by counting the number of brown positive cells/total number of cells×100. This was performed manually. This was repeated twice to ensure that intraobserver variability was $<10\%$.

Micro-computed tomography analysis for the vasa vasorum of the jugular vein

Three-dimensional microscopic computed tomography was performed to determine the presence of the vasa vasorum in the jugular vein of a C57Bl/6 mouse, as previously described.[45] A representative figure is provided in Supplementary Figure S4 online.

Statistical methods

Data are expressed as mean ± s.e.m. Multiple comparisons were performed with two-way analysis of variance followed by Student's *t*-test with *post hoc* Bonferroni's correction. We used Kaplan–Meier survival model to assess for differences in patency between groups. A log-rank test was performed. Significant difference from control value was indicated by $^{*}P<0.05$, $^{**}P<0.001$, or $^{\#}P<0.0001$ for *in vitro* experiments and $^{*}P<0.01$, $^{**}P<0.001$, or $^{\#}P<0.0001$ for *in vivo* experiments. For comparison of gene expression for *VEGF-A* in Avastin-treated vessels compared with controls only, a paired Student's *t*-test was performed with significance at $P<0.05$. JMP version 9 (SAS Institute, Cary, NC) was used for statistical analyses.

DISCLOSURE

All the authors declared no competing interests.

ACKNOWLEDGMENTS

We are grateful to Dr Nagy (University of Toronto) for providing us the probe for the *in situ* hybridization experiments. This work was funded by R01HL098967 (to SM) from the National Heart, Lung, and Blood Institute.

SUPPLEMENTARY MATERIAL

Figure S1. LV-shRNA-VEGF-A transfection decreases *VEGF-A* expression in cells.
Figure S2. Hematoxylin and eosin (H and E) and picrosirius red staining of the LV-shRNA-*VEGF-A*-transfected vessels and control vessels.
Figure S3. Vimentin staining shows no difference in LV shRNA–transduced vessels when compared with controls
Figure S4. Micro-CT analysis of a mouse jugular vein.
Supplementary material is linked to the online version of the paper at http://www.nature.com/ki

REFERENCES

1. Collins AJ, Kasiske B, Herzog C *et al.* Excerpts from the United States Renal Data System 2003 Annual Data Report: atlas of end-stage renal disease in the United States. *Am J Kidney Dis* 2003; **42**: A5–A7.
2. Rooijens PPGM, Tordoir JHM, Stijnen T *et al.* Radiocephalic wrist arteriovenous fistula for hemodialysis: meta-analysis indicates a high primary failure rate. *Eur J Vasc Endovasc Surg* 2004; **28**: 583–589.
3. Sullivan KL, Besarab A, Bonn J *et al.* Hemodynamics of failing dialysis grafts. *Radiology* 1993; **186**: 867–872.
4. Rekhter M, Nicholls S, Ferguson M *et al.* Cell proliferation in human arteriovenous fistulas used for hemodialysis. *Arterioscler Thromb* 1993; **13**: 609–617.
5. Swedberg SH, Brown BG, Sigley R *et al.* Intimal fibromuscular hyperplasia at the venous anastomosis of PTFE grafts in hemodialysis patients. Clinical, immunocytochemical, light and electron microscopic assessment. *Circulation* 1989; **80**: 1726–1736.
6. Roy-Chaudhury P, Kelly BS, Miller MA *et al.* Venous neointimal hyperplasia in polytetrafluoroethylene dialysis grafts. *Kidney Int* 2001; **59**: 2325–2334.
7. Misra S, Doherty MG, Woodrum D *et al.* Adventitial remodeling with increased matrix metalloproteinase-2 activity in a porcine arteriovenous polytetrafluoroethylene grafts. *Kidney Int* 2005; **68**: 2890–2900.
8. Li L, Terry CM, Blumenthal DK *et al.* Cellular and morphological changes during neointimal hyperplasia development in a porcine arteriovenous graft model. *Nephrol Dial Transplant* 2007; **22**: 3139–3146.
9. Wang Y, Krishnamoorthy M, Banerjee R *et al.* Venous stenosis in a pig arteriovenous fistula model anatomy, mechanisms and cellular phenotypes. *Nephrol Dial Transplant* 2007; **22**: 3139–3146.
10. Janardhanan R, Yang B, Vohra P *et al.* Simvastatin reduces venous stenosis formation in a murine hemodialysis vascular access model. *Kidney Int* 2013; **84**: 338–352.
11. Misra S, Fu A, Rajan D *et al.* Expression of hypoxia inducible factor-1 alpha, macrophage migration inhibition factor, matrix metalloproteinase-2 and -9, and their inhibitors in hemodialysis grafts and arteriovenous fistulas. *J Vasc Interv Radiol* 2008; **19**: 252–259.
12. Misra S, Fu A, Anderson J *et al.* The rat femoral arteriovenous fistula model: increased expression of MMP-2 and MMP-9 at the venous stenosis. *J Vasc Interv Radiol* 2008; **19**: 587–594.
13. Misra S, Fu AA, Puggioni A *et al.* Increased shear stress with up regulation of VEGF-A and its receptors and MMP-2, MMP-9, and TIMP-1 in venous stenosis of hemodialysis grafts. *Am J Physiol Heart Circ Physiol* 2008; **294**: H2219–H2230.
14. Misra S, Shergill U, Yang B *et al.* Increased expression of HIF-1α, VEGF-A and its receptors, MMP-2, TIMP-1, and ADAMTS-1 at the venous stenosis of arteriovenous fistula in a mouse model with renal insufficiency. *J Vasc Interv Radiol* 2010; **21**: 1255–1261.
15. Bhardwaj S, Roy H, Heikura T *et al.* VEGF-A, VEGF-D and VEGF-D induced intimal hyperplasia in carotid arteries. *Eur J Clin Invest* 2005; **35**: 669–676.
16. Di Marco GS, Reuter S, Hillebrand U *et al.* The soluble VEGF receptor sFlt1 contributes to endothelial dysfunction in CKD. *J Am Soc Nephrol* 2009; **20**: 2235–2245.
17. Hutter R, Carrick FE, Valdiviezo C *et al.* Vascular endothelial growth factor regulates reendothelialization and neointima formation in a mouse model of arterial injury. *Circulation* 2004; **110**: 2430–2435.
18. Inoue M, Itoh H, Ueda M *et al.* Vascular endothelial growth factor (VEGF) expression in human coronary atherosclerotic lesions: possible pathophysiological significance of VEGF in progression of atherosclerosis. *Circulation* 1998; **98**: 2108–2116.
19. Simons M. VEGF and restenosis: the rest of the story. *Arterioscler Thromb Vasc Biol* 2009; **29**: 439–440.
20. Shiojima I, Walsh K. The role of vascular endothelial growth factor in restenosis: the controversy continues. *Circulation* 2004; **110**: 2283–2286.
21. Zhao Q, Egashira K, Hiasa K *et al.* Essential role of vascular endothelial growth factor and Flt-1 signals in neointimal formation after periadventitial injury. *Arterioscler Thromb Vasc Biol* 2004; **24**: 2284–2289.
22. Ohtani K, Egashira K, Hiasa K-i *et al.* Blockade of vascular endothelial growth factor suppresses experimental restenosis after intraluminal injury by inhibiting recruitment of monocyte lineage cells. *Circulation* 2004; **110**: 2444–2452.
23. Yang B, Shergill U, Fu AA *et al.* The mouse arteriovenous fistula model. *J Vasc Interv Radiol* 2009; **20**: 946–950.
24. Misra S, Shergill U, Yang B *et al.* Increased expression of HIF-1alpha, VEGF-A and its receptors, MMP-2, TIMP-1, and ADAMTS-1 at the venous stenosis of arteriovenous fistula in a mouse model with renal insufficiency. *J Vasc Interv Radiol* 2010; **21**: 1255–1261.

25. Shay-Salit A, Shushy M, Wolfovitz E *et al.* VEGF receptor 2 and the adherens junction as a mechanical transducer in vascular endothelial cells. *Proc Natl Acad Sci USA* 2002; **99**: 9462–9467.
26. Wang H, Keiser JA. Vascular endothelial growth factor upregulates the expression of matrix metalloproteinases in vascular smooth muscle cells: role of flt-1. *Circ Res* 1998; **83**: 832–840.
27. Misra S, Fu AA, Misra KD *et al.* Hypoxia-induced phenotypic switch of fibroblasts to myofibroblasts through a matrix metalloproteinase 2/tissue inhibitor of metalloproteinase-mediated pathway: implications for venous neointimal hyperplasia in hemodialysis access. *J Vasc Interv Radiol* 2010; **21**: 896–902.
28. Das M, Burns N, Wilson SJ *et al.* Hypoxia exposure induces the emergence of fibroblasts lacking replication repressor signals of PKC{zeta} in the pulmonary artery adventitia. *Cardiovasc Res* 2008; **78**: 440–448.
29. Misra S, Fu A, Pugionni A *et al.* Increased expression of hypoxia inducible factor-1α in a porcine model of chronic renal insufficiency with arteriovenous polytetrafluoroethylene grafts. *J Vasc Interv Radiol* 2008; **19**: 260–265.
30. Misra S, Bonan R, Pflederer T *et al.* BRAVO I: a pilot study of vascular brachytherapy in polytetrafluoroethylene dialysis access grafts. *Kidney Int* 2006; **70**: 2006–2013.
31. Haskal ZJ, Trerotola S, Dolmatch B *et al.* Stent graft versus balloon angioplasty for failing dialysis-access grafts. *N Engl J Med* 2010; **362**: 494–503.
32. Abbruzzese TA, Guzman RJ, Martin RL *et al.* Matrix metalloproteinase inhibition limits arterial enlargements in a rodent arteriovenous fistula model. *Surgery* 1998; **124**: 328–334.
33. Rotmans JI, Velema E, Verhagen HJ *et al.* Matrix metalloproteinase inhibition reduces intimal hyperplasia in a porcine arteriovenous-graft model. *J Vasc Surg* 2004; **39**: 432–439.
34. Wang H, Zhang M, Bianchi M *et al.* Fetuin (alpha 2-HS-glycoprotein) opsonizes cationic macrophagedeactivating molecules. *Proc Natl Acad Sci USA* 1998; **95**: 14429–14434.
35. Kokubo T, Ishikawa N, Uchida H *et al.* CKD accelerates development of neointimal hyperplasia in arteriovenous fistulas. *J Am Soc Nephrol* 2009; **20**: 1236–1245.
36. Pawlak K, Pawlak D, Mysliwiec M. Circulating beta-chemokines and matrix metalloproteinase-9/tissue inhibitor of metalloproteinase-1 system in hemodialyzed patients–role of oxidative stress. *Cytokine* 2005; **31**: 18–24.
37. Pawlak K, Pawlak D, Mysliwiec M. Possible association between circulating vascular endothelial growth factor and oxidative stress markers in hemodialysis patients. *Med Sci Monit* 2006; **12**: CR181–CR185.
38. Pawlak K, Pawlak D, Mysliwiec M. Serum matrix metalloproteinase-2 and increased oxidative stress are associated with carotid atherosclerosis in hemodialyzed patients. *Atherosclerosis* 2007; **190**: 199–204.
39. Esposito C, He CJ, Striker GE *et al.* Nature and severity of the glomerular response to nephron reduction is strain-dependent in mice. *Am J Pathol* 1999; **154**: 891–897.
40. Wang Y, Wang YP, Tay YC *et al.* Progressive adriamycin nephropathy in mice: sequence of histologic and immunohistochemical events. *Kidney Int* 2000; **58**: 1797–1804.
41. Bock F, Onderka J, Dietrich T *et al.* Bevacizumab as a potent inhibitor of inflammatory corneal angiogenesis and lymphangiogenesis. *Invest Ophthalmol Vis Sci* 2007; **48**: 2545–2552.
42. *Committee on Care and Use of Laboratory Animals of the Institute of Laboratory Animal Resources*. Government print office: Washington, DC, 1996.
43. Turunen MP, Lehtola T, Heinonen SE *et al.* Efficient regulation of VEGF expression by promoter-targeted lentiviral shRNAs based on epigenetic mechanism: a novel example of epigenetherapy. *Circ Res* 2009; **105**: 604–609.
44. Basu S, Nagy JA, Pal S *et al.* The neurotransmitter dopamine inhibits angiogenesis induced by vascular permeability factor/vascular endothelial growth factor. *Nat Med* 2001; **7**: 569–574.
45. Hughes D, Fu AA, Puggioni A *et al.* Adventitial transplantation of blood outgrowth endothelial cells in porcine haemodialysis grafts alleviates hypoxia and decreases neointimal proliferation through a matrix metalloproteinase-9-mediated pathway–a pilot study. *Nephrol Dial Transplant* 2009; **24**: 85–96.